Published in final edited form as:

Nat Rev Chem. 2022 June ; 6(6): 405–427. doi:10.1038/s41570-022-00388-4.

Radical C(sp3)–H functionalization and cross-coupling reactions

Dung L. Golden[1,2], **Sung-Eun Suh**[1,2,3], **Shannon S. Stahl**[1,*]

[1]Department of Chemistry, University of Wisconsin–Madison, WI, USA.

[2]These authors contributed equally: Dung L. Golden, Sung-Eun Suh.

[3]Department of Chemistry, Ajou University, Suwon, Republic of Korea

Abstract

C—H functionalization reactions are playing an increasing role in the preparation and modification of complex organic molecules, including pharmaceuticals, agrochemicals, and polymer precursors. Radical C—H functionalization reactions, initiated by hydrogen-atom transfer (HAT) and proceeding via open-shell radical intermediates, have been expanding rapidly in recent years. These methods introduce strategic opportunities to functionalize C(sp^3)—H bonds. Examples include synthetically useful advances in radical-chain reactivity and biomimetic radical-rebound reactions. A growing number of reactions, however, proceed via "radical relay" whereby HAT generates a diffusible radical that is functionalized by a separate reagent or catalyst. The latter methods provide the basis for versatile C—H cross-coupling methods with diverse partners. In the present review, highlights of recent radical-chain and radical-rebound methods provide context for a survey of emerging radical-relay methods, which greatly expand the scope and utility of intermolecular C(sp^3)—H functionalization and cross coupling.

Graphical Abstract

* stahl@chem.wisc.edu .

Author contributions

D.L.G. and S.-E.S. contributed equally to all aspects of the review. D.L.G., S.-E.S., and S.S.S wrote, edited, and reviewed the manuscript.

Competing interests statement

The authors declare no competing interests.

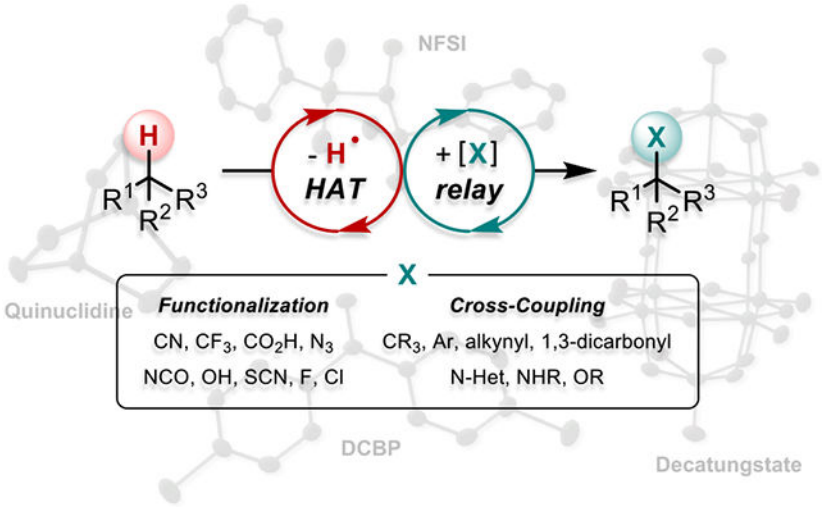

Radical reaction pathways have evolved sufficiently that C(sp^3)—H bonds may now be viewed as strategic "reagents" for bond formation in synthetic organic chemistry. This Review highlights the diverse approaches for C(sp^3)–H functionalization and cross-coupling reactions, emphasizing radical-relay reactions.

Introduction

Efficient synthesis of organic molecules is crucial to drug discovery and development, materials synthesis, and many other domains. C—H functionalization methods provide a means to streamline synthetic routes by avoiding substrate preactivation, accessing target molecules in fewer steps, and providing efficient strategies to diversify existing chemical structures, including modification of their physicochemical properties and three-dimensional structures. Multiple mechanistic pathways are available for C(sp^3)—H functionalization, including those initiated by organometallic C—H activation[1-4]; atom-transfer methods[5-7], such as carbene and nitrene C—H insertion; and those initiated by hydrogen-atom transfer (HAT) to generate radical intermediates[4,8-10]. The synthetic utility of radical C—H functionalization reactions was historically viewed with skepticism[11], owing to the challenges in controlling reaction selectivity; however, recent advances have changed this perception. Radical pathways are featured in a growing number of synthetically useful methods that enable site-selective functionalization of C(sp^3)—H bonds. C—H functionalization reactions that feature a one-for-one replacement of a hydrogen atom with another functional group, such as a halogen, pseudohalogen, or oxygen atom, have been complemented by C—H cross-coupling reactions that permit efficient access to dozens, if not hundreds, of derivatives via reaction of the C—H substrate with broad classes of reaction partners, such as aryl halides, boronic acids, alcohols, and amine derivatives. The latter reactions represent an important class of reactions for pharmaceutical and agrochemical discovery efforts due to their ability to enable rapid elaboration of simple building blocks, core structures of moderate complexity, and late-stage structures and bioactive compounds.

Multiple mechanisms are available for radical C—H functionalization reactions. Radical-chain mechanisms (FIG. 1Aa) are involved in a number of large-scale industrial processes,

including chlorination of methane and autoxidation of hydrocarbons, such as cyclohexane and cumene[12,13]. These reactions feature three general steps: initiation, propagation, and termination. The initiation step generates new radical species, typically by thermal or photochemical cleavage of a weak bond in dihalogens (e.g., Cl_2 and Br_2), peroxides, or specialized reagents, such as such as AIBN (2,2'-azobis(2-methylpropionitrile). Propagation steps account for net transformation of the starting material into the reaction product(s). These steps regenerate the radical carrier without net consumption of radical species. The chain process ends in termination steps that consume radicals, such as the direct coupling of two radicals. Recent advances have highlighted the utility of radical-chain reactions for selective functionalization of more complex molecules, benefiting from the development of new reagents that lead to improved site selectivity in the HAT propagation step[14-17].

The radical-rebound mechanism (FIG. 1Ba) is closely associated with iron-containing heme enzymes such as cytochrome P450 (CYP) and related non-heme iron enzymes in biology[18]. This collection of biological and synthetic reactions involves high-valent metal-oxo species generated via reaction of a reduced metal complex with oxygen-atom donors, including O_2, H_2O_2, alkyl or acyl hydroperoxides, and PhI=O. HAT from a C(sp^3)—H bond to the reactive metal-oxo is followed by rapid recombination (i.e., rebound) of the resulting carbon-centered radical with the incipient metal-hydroxide to afford the oxygenated product. Variations of this reaction pathway can lead to other products if the organic radical recombines with a different ligand within the metal coordination sphere. For example, C—H halogenation products can arise from HAT by a metal oxo, followed by reaction of the organic radical with a halide ligand rather than the hydroxide ligand. Analogous C—H amination reactivity is possible with metal-nitrene intermediates derived from the reaction of a reduced metal complex with nitrogen-atom donors, including organic azides[19] and PhI=NR reagents[20]. Recent advances include the discovery of new catalysts that promote radical-rebound reactions with complex molecules.

Radical-relay reactions (FIG. 1C) complement radical-chain and radical-rebound reactions and significantly expand the scope of accessible synthetic transformations. An HAT step generates a diffusible organic radical, which is then functionalized by a second reagent or catalyst. In some cases, the radical undergoes direct coupling with a substrate partner or radical trapping reagent (FIG. 1Ca). In other cases, the radical undergoes metal-catalyzed coupling, reacting by one of several possible mechanisms (FIG. 1Cb). It can undergo radical-polar crossover, in which electron-transfer (ET) generates a carbocation that reacts readily with diverse nucleophiles. Alternatively, the carbon-centered radical can react by one of two possible pathways with a transition-metal catalyst containing Ni^{II}, Cu^{II}, or another metal ion: (a) direct addition of the radical to a coordinated ligand on the transition-metal complex, or (b) radical addition to the metal center and subsequent reductive elimination with the coordinated coupling partner. Each of these pathways support C—H cross-coupling reactions that generate new carbon-carbon and carbon-heteroatom bonds via reaction with diverse reaction partners. Recent advances have introduced new methods to access HAT reagents from chemical oxidants and photoactive reagents, in addition to new catalyst systems that support diverse product formation.

The intermolecular C(sp^3)—H functionalization and cross-coupling methods represented by these reaction classes provide valuable strategies to diversify organic molecules ranging from simple building blocks to complex molecules[21-23]. Intramolecular reactions, such as Hoffmann-Loeffler-Freitag and related reactions[24-26], feature closely related mechanisms but are outside the synthetic scope of this review. The content herein begins with a survey of new radical-chain and radical-rebound reactions, followed by a presentation of radical-relay reactions that use C—H bonds as latent nucleophiles in carbon—carbon and carbon–heteroatom bond-forming reactions. Cross-coupling methods include those that feature direct C—H cross coupling, in addition to those that proceed via stepwise C—H functionalization/diversification sequences. Mechanistic features of these reactions are presented, emphasizing those with implications for the synthetic scope of the reactions.

Radical-chain and radical-rebound reactions

Radical chain.

Conventional radical-chain reactions involving Cl_2 and Br_2 often lack the selectivity required to support synthetically useful, site-selective C—H functionalization of complex molecules. Over the past decade, however, a number of N—X (X = F, Cl) reagents have been shown to promote radical-chain C—H fluorination and chlorination with improved yields and selectivity (FIG. 2Aa). *N*-Fluorobenzenesulfonimide (NSFI) and Selectfluor reagents are featured in a number of C(sp^3)—H fluorination methods, and they have been paired with various initiators, including azobisisobutyronitrile (AIBN)[27], BEt_3/O_2[28], and copper(I)[29] (FIG. 2Ab, condition 1). Reactions using $Fe(acac)_2$/Selectfluor[30] (acac = acetylacetonate) and CuOAc/NFSI[31] support selective fluorination of benzylic C—H bonds and the reactivity is consistent with a radical-chain pathway. A multicomponent Cu(bis-imine)/Selectfluor/*N*-hydroxyphthalimide (NHPI) catalyst system with $KB(C_6F_5)_4$ as an anionic phase-transfer catalyst supports fluorination of stronger aliphatic C—H bonds[32]. N—F reagents have also been paired with photocatalysts, including diarylketone[33] and tetrabutylammonium decatungstate (TBADT)[27,34]. These reagents are capable of promoting HAT from C—H substrates (FIG. 2Ab, condition 2 and 3), and the resulting carbon-centered radicals can react with fluorinating reagents to afford the desired C—F bonds. It is possible that HAT could proceed via both radical-chain and photocatalyst-promoted steps in these reactions. Fluorination of benzylic C(sp^3)—H bonds has been achieved using 1,2,4,5-tetracyanobenzene, although this photocatalyst is proposed to initiate an electron transfer pathway[35]. Collectively, these methods provide effective routes to monofluorinated benzylic and aliphatic C(sp^3)—H products. The reactions show good selectivity for benzylic C—H bonds in the photocatalyzed (e.g., diaryl ketone, TBADT) and metal-initiated radical chains. Difluorination can be achieved under more forcing condition and by employing additional Selectfluor and diaryl ketone as photocatalyst[33].

Complementary reagents have been developed to support selective radical-chain chlorination. A sterically encumbered *N*-chloroamide reagent supports chlorination of aliphatic C(sp^3)—H substrates under visible-light irradiation, taking advantage of difference in electronics and sterics of various C—H bonds to achieve improved selectivity relative to conventional chlorination methods (FIG. 2Ac, X = Cl)[14]. Steric modulation of aryl

ring of the *N*-chloroamide reagent, by shifting two trifluoromethyl groups from meta to ortho positions with respect to the carbonyl group, alters regioselectivity in the chlorination of aliphatic C—H bonds[36]. A sterically hindered, 2,2,6,6-tetramethylpiperidinium N—Cl reagent (cf. FIG. 1Ab) is an effective chlorinating reagent and chain carrier for photoinitiated C—H chlorination[37]. The electrophilicity and steric hindrance of the aminium radical confers excellent selectivity in reactions with less sterically hindered methylene C—H sites and with weaker tertiary C(sp^3)—H bonds. Radical-chain chlorination of primary or secondary benzylic C—H bonds with *N*-chlorosuccinimide (NCS) has been initiated by reductive activation of NCS with an acridinium-based photocatalyst to generate a nitrogen-centered radical[38]. In addition to N–Cl reagents, *tert*-butyl hypochlorite (*t*BuOCl) has been used with a phenanthroline (phen)-ligated silver catalyst to chlorinate C(sp^3)—H bonds[39]. The reaction has been proposed to proceed via silver-mediated C—Cl bond formation; however, a radical-chain pathway could also account for the observed reactivity. In the latter pathway, a carbon-centered radical generated by HAT could react via chain propagation with *t*BuOCl.

Radical-chain reactions have been developed for selective conversion of C(sp^3)—H bonds into C—Br, C—S, and C—O bonds. Variants of the *N*-chloroamide reagent in FIG 2Ac in which N—Cl is replaced with N—Br or N—xanthyl (xanthyl = −S(C=S)OEt) supports C—H bromination[15] and xanthylation[16], respectively. Xanthylated products are versatile intermediates in two-step C—H functionalization/diversification reactions in which the xanthyl group may be displaced in a second step by other groups, including allyl, vinyl, CF_3, D, NR_2, N_3, OH, and SR (FIG. 2Ac)[16,40]. Bis(methanesulfonyl) peroxide supports radical-chain C—H oxygenation of benzylic C(sp^3)—H bonds in the presence of a copper(I) initiator, and the resulting benzyl mesylates undergo facile displacement by water in the presence of hexafluoroisopropanol (HFIP) to afford benzyl alcohols (FIG. 2Ad).[17]

Collectively, these synthetic methods and reagents highlight the emergence of numerous synthetically useful radical-chain reactions. Sterically and electronically tailored N—X and O—X reagents (X = heteroatom substituent) have begun to overcome historical limitations of radical-chain reactions involving simple Cl_2, Br_2, and related reagents. Moreover, recent applications of radical-chain reactivity have demonstrated the ability to employ C—H substrates as the limiting reagent and exhibit good site selectivity and compatibility with functional groups that are sensitive to polar reagents.

Radical rebound.

Radical-rebound C(sp^3)—H functionalization takes inspiration from heme and non-heme iron oxygenase enzymes[18,41]. Early studies of model complexes for non-heme iron enzymes investigated reactions with hydrogen peroxide as the oxidant and provided clear evidence for generation of high-valent iron-oxo species[42-46]. For example, stereospecificity observed in the hydroxylation of alkanes supports rapid rebound of the organic radical with an intermediate Fe—OH species generated via HAT (cf. FIG 1Ba)[46-4748]. These and related studies established a foundation for more recent synthetic applications of this reactivity using similar catalyst systems. Nitrogen-ligated iron catalysts have been developed for stereo- and site-selective oxidation of aliphatic C—H bonds in molecules containing

multiple secondary and tertiary C—H bonds[49]. The C—H substrate is used as the limiting reagent in these reactions, distinguishing these reactions from the earlier studies, which used excess hydrocarbon substrate with limiting oxidant. Electronic, steric, and stereoelectronic factors contribute to site selectivity,[50] with reactivity favored at electron-rich and less hindered sites, in addition to sites that relieve strain in the HAT step[51,52]. These catalyst systems have been implemented for hydroxylation of structurally complex molecules[49,52-54], and modification of the ligand structure allows for enhanced and/or altered site-selectivity (FIG. 2B). Manganese catalysts analogous to the Fe-based catalyst systems have also been employed in synthetically important radical-rebound oxygenation reactions[55-57]. Enantioselective oxidation of methylene C—H bonds has been achieved by using a chiral tetradentate nitrogen ligand to support enantioselective HAT (FIG. 2Ca)[58]. Carboxylic acid additives contribute significantly to the reaction outcome by promoting O—O bond cleavage of the hydroperoxide intermediate to afford the reactive metal-oxo species and by replacing a metal-bound hydroxide with a carboxylate ligand that influences both site-selectivity and enantioselectivity in C—H oxidation reactions[49,51-54,58-61].

Various manganese-based catalysts show that the radical-rebound pathway can provide the basis for aliphatic C(sp^3)—H functionalization beyond oxygenation (FIG. 2Cb). Mn-porphyrin and Mn-salen complexes support chemoselective halogenation (fluorination, chlorination)[62-65] and pseudohalogenation, with azide[66]and isocyanate[67] sources. Most of these reactions employ iodosylbenzene (PhIO) as the oxidant. The radical-rebound mechanism is not limited to oxygen-centered HAT species. A Mn-phthalocyanine catalyst supports sulfonamidation of benzylic C(sp^3)—H bonds using a trichloroethoxysulfonamide-derived hypervalent iodine reagent (PhI=NTces)[20] (FIG 2Cb). The reaction is highly selective for benzylic sites in the presence of other aliphatic C—H bonds and exhibits good functional group tolerance. These efforts showcase synthetically useful applications of the radical-rebound mechanism to achieve site-selective carbon-heteroatom bond forming reactions.

Radical-relay reactions involving direct coupling with a substrate partner or radical trapping reagent

The development of radical-relay reactions in recent years has significantly expanded the scope of C(sp^3)—H functionalization. The term "radical relay" is used here to describe non-chain radical C—H functionalization reactions in which the HAT species does not incorporate the group or reagent that undergoes coupling with the intermediate organic radical (cf. FIG. 1). The first class of radical-relay reactions, summarized in this section, feature direct addition of an organic radical to a trapping reagent or coupling partner. The HAT species used to generate the organic radical may be generated one of several different pathways, including redox processes that lead to generation an oxyl radical (e.g., via oxidation of an O—H bond or reductive cleavage of an N—O bond); photochemical excitation of decatungstate anion or aryl ketones; photon-induced ligand-to-metal charge transfer of a transitional metal reagent, resulting in homolytic cleavage of a M—OR or M—Cl bond; reductive activation of N—F reagents, such as NFSI or Selectfluor reagents; among others.

Radical-relay C—H oxygenation reactions may be achieved by combining an HAT reagent with O_2 or another oxygen-atom source as the radical trap[4,68,69]. These methods often exhibit improved selectivity relative to conventional autoxidation methods. A prominent example of this concept features the use of *N*-hydroxyphthalimide (NHPI), which generates the HAT species phthalimido-*N*-oxyl (PINO) in the presence of O_2 and a cobalt catalyst (FIG. 3Aa)[70,71]. PINO-mediate HAT from weak C(sp^3)—H bonds generates a carbon-centered radical that reacts rapidly with O_2, ultimately affording ketones, carboxylic acids, or other oxygenation products. This reactivity was initially demonstrated with simple hydrocarbons[70], but it has recently been applied to oxygenation of heterobenzylic C—H bonds in pharmaceutically relevant building blocks[71]. The scope of alkylated heterocycles was extended by the development of an iron, rather than cobalt, cocatalyst[72]. The oxygenation of methylarenes under Co/NHPI/O_2 conditions typically generates benzoic acid derivatives; however, the use of an HFIP solvent system enables selective formation of benzyaldehydes. Hydrogen bonding from HFIP is proposed to polarize the carbonyl group of the aldehyde to prevent further oxidation to benzoic acid[73]. Decatungstate (DT) photocatalysts serve as an effective HAT reagent upon near-ultraviolet irradiation, and they support reactivity at C(sp^3)—H bonds stronger that those typically reactive with PINO. The excited-state DT species is an electrophilic HAT reagent, and protonated amines undergo reaction at C—H bonds remote from the electron-withdrawing ammonium group, forming ketones in the presence of H_2O_2 (FIG. 3Ab)[74]. TBADT has been used as an HAT photocatalyst to support oxygenation of (hetero)benzylic and aliphatic C—H bonds in the presence of O_2 under batch[75] and continuous flow[76] conditions.

PINO is a meta-stable radical, and, in addition to serve as an HAT reagent, it can trap carbon-centered radicals to afford PINOylated products (FIG. 3B). This reactivity has been achieved by combining catalytic copper(I) chloride, (diacetoxyiodo)benzene ($PhI(OAc)_2$), and NHPI with the C—H substrate (FIG. 3Ba)[77]. Similar reactivity has been achieved with a reaction system comprising catalytic copper(II) acetate, Selectfluor, and NHPI (FIG. 3Bb)[78]. The mechanism of these reactions is not well understood, but reactive HAT species could be generated by oxidation of NHPI or reductive activation of the stoichiometric oxidant, and the Cu catalyst could contribute to each of these processes. Ultimately, the PINOylation product may be formed by coupling of the carbon-centered radical derived from HAT with PINO.

Sulfonyl–X reagents (X = N_3, CN, SR, SCF_3, SePh, Cl, $CH{=}CHSO_2Ph$, and C≡Ar) react with carbon-centered radicals to afford C—X bonds, and they are employed in a number of radical-relay C(sp^3)—H functionalization reactions. Various methods may be used to generate the radical via HAT from an C(sp^3)—H bond. Azidation of aliphatic C—H bonds can proceed under metal-free conditions, using potassium persulfate as the HAT precursor with an arylsulfonyl azide trapping reagent (FIG. 3Ca)[79]. Photoexcited decatungstate has been used to promote HAT in the presence of tosyl cyanide to support C—H cyanation (FIG. 3Ca, bottom)[80]. DT-mediated HAT has also been used other radical traps, including sulfur dioxide[81], (trifluoromethylthio)phthalimide[82], and other sulfonyl–X reagents (e.g., methanesulfonyl alkynes[83]) to achieve C—H functionalization. Reductive activation of the N—F reagent *N*-(tert-butyl)-*N*-fluoro-3,5-bis(trifluoromethyl)benzene-sulfonamide by copper(I) has been used to generate a nitrogen-centered radical capable of promoting HAT in the presence of $PhSO_2$–X reagents (X = SCF_3, SePh, C≡CPh, CN, N_3, Cl, $CH{=}CHSO_2Ph$).

This reactivity was most extensively demonstrated for thiolation of C(sp^3)—H bonds (FIG. 3Cb)[84]. This chemistry is closely related to Cu/NFSI-based C—H functionalization methods elaborated below, with the distinction that the carbon-centered radical intermediate directly adds to the sulfonyl–X reagent rather than undergoing Cu-catalyzed functionalization (see FIG. 1Ca/b and content below for additional context).

Dialkyl azodicarboxylate reagents react as radical traps to support amination of C(sp^3)—H bonds. A copper(II)/organic HAT catalyst system using diethyl azodicarboxylate (DEAD) has been used to achieve site selective amination of heterobenzylic C(sp^3)—H bonds (FIG. 3Da)[85]. Copper(II) acts as a Lewis acid catalyst to enhance the reactivity of heterobenzylic positions, leading to high selectivity in presence of weaker benzylic C—H bonds. Photoinduced ligand-to-metal charge transfer (LMCT) in cerium(IV)–X reagents has been use to generate reactive heteroatom-based radicals that promote HAT from C(sp^3)—H bonds. The initial reports proposed formation of an oxygen-centered radical via LMCT within a cerium(IV)-alkoxide complex[86,87]; however, a subsequent study implicated the formation of chlorine radical via LMCT involving a Ce^{IV}—Cl fragment[88]. In both proposed mechanisms, the heteratom radical promotes HAT, and the resulting carbon-centered radical adds to the dialkyl azodicarboxylate reagent to form a C—N bond. This steps leads to formation of an adjacent nitrogen-centered radical that is proposed to be reduced by cerium(III) and undergo protonation to afford the final product (FIG. 3Db)[87]. The N—N bond is subjected to hydrogenolysis over Raney Ni to afford the primary amine derivative. DT photocatalysis has also been used to support HAT from C—H bonds in the presence of dialkyl azodicarboxylate to afford the C—N coupling products[89,90]. A photoreactor with high intensity LED light has been used to achieve this reactivity under flow conditions[91].

Electron-deficient alkenes can serve as radical traps that provide the basis for C(sp^3)—H alkylation. The addition to carbon-centered radicals to alkenes ("Giese reactions"[92-94]) generates a new carbon-centered radical that can react with a hydrogen-atom donor (e.g., a thiol or other reagnet) or undergo one-electron reduction and protonation to afford the alkylate product. Light-promoted LMCT from copper(II)[95], cerium(IV)[86,87], and iron(III)[96] reagents and DT photocatalysts[97-100] have been used to generate reactive species that support HAT from the C—H substrate. A DT-catalyzed Giese-type radical addition reaction was implemented in continuous flow to forge new C(sp^3)—C(sp^3) bonds between light alkanes, including methane, ethane, propane, and isobutane, and electron-deficient alkenes (FIG. 3Ea)[101]. HAT reagents typically consist of electrophilic radicals that favor reaction at electron-rich C—H bonds (e.g., 3° aliphatic and benzylic C—H bonds); however, polarity-reversed HAT[102] from acidic C—H bonds adjacent to electron-withdrawing groups was enabled by using an amine-borane catalyst under photochemical conditions (FIG. 3Eb)[103]. The organic radical subsequently adds to an unactivated alkene followed by abstracting a hydrogen atom from a thiol-based H-atom donor to afford the C(sp^3)—C(sp^3) coupling product.

Electron-deficient arenes and heterocycles, such as pyridinium groups, also react readily with nucleophilic radicals ("Minisci reactions"[104,105]). This reactivity may be used to support (hetero)arylation of C(sp^3)—H bonds by generating carbon-centered radicals via HAT. Representative HAT reagents that have been used in Minisci-type

coupling reactions include oxygen-and nitrogen-centered radicals derived from peroxides/alcohols and amides[106-109], DT photocatalysts[110-113], azide radical[114], and hypervalent iodine[114]. For example, a ruthenium photoredox catalyst can undergo SET with hydroxyl perfluorobenziodoxole (PFBI–OH) to generate an oxygen-centered radical[114]. HAT generates a carbon-centered radical that adds to a protonated *N*-heteroarene, and subsequent loss of an electron and proton from the adduct affords the Minisci coupling product (FIG. 3Fa). In another example, anthraquinone proved superior to TBADT and benzoquinone as a photocatalyst/HAT reagent in the direct coupling of alkanes with *N*-aminopyridinium salts[115]. The radical adds to the electron-deficient heterocycle, similar to Minisci reactions, with C4 selectivity (FIG. 3Fb). The reaction employs 5 equiv of alkane, aldehyde, and other coupling partners (e.g., P—H, Si-H substrates).

A primary-selective C—H borylation is initiated by photoinduced electron transfer upon irradiating *N*-(trifluoroethoxy)phthalimide in the presence of bis(catecholato)diboron (B_2cat_2), 10 equiv of the C—H substrate, and 20 mol% *B*-chlorocatecholborane [ClB(cat)] (FIG. 3G)[116]. Mesolytic cleavage of the N—O bond affords a trifluoroethoxy radical that is proposed to react with ClB(cat) to generate the reactive HAT species. The lack of a photoredox catalyst supports radical, rather than radical-polar crossover, reactivity. Carbon-boron bond formation arises from reaction of the intermediate organic radical with B_2cat_2. High primary C—H selectivity, even in the presence of weaker secondary tertiary C—H bonds, is rationalized by the involvement of a chlorine radical–boron ‘ate’ complex that selectively cleaves sterically unhindered C—H bonds.

Kharasch-Sosnovsky reactions: Early examples of catalytic radical relay

The Kharasch-Sosnovsky (K-S) allylic oxidation reaction, first reported in 1958, represents a seminal precedent for catalytic radical-relay reactivity (FIG. 1Cb)[117,118]. The original transformation used copper(I) bromide and *tert*-butyl peroxybenzoate (TBPB) to achieve allylic oxidation of cyclohexene, 1-hexene, and 1-octene, affording the allylic benzoate derivatives (FIG. 4a). The proposed mechanism involves Cu^{I}-mediated activation of the peroxide, allylic HAT by *t*BuO• and coupling of the allylic radical with Cu^{II}-benzoate (FIG. 4b)[119]. Asymmetric C—O coupling, which was initially achieved by using a catalytic amount of L-proline as a chiral ligand (40% yield, 30% ee)[120], implicates inner-sphere coupling of the C—O bond via radical addition to Cu^{II} and C—O reductive elimination (FIG. 4c). Improved enantioselectivity was achieved by using chiral bis- or trisoxazoline ligands (FIG. 4e)[121–124]. Most K-S reactions use excess C—H substrate relative to the peroxide reagent. Low temperatures (e.g., −20 °C) are needed to enhance enantioselectivity, but these conditions often result in multiple-day reaction times. K-S oxidation methods have been used in synthetic chemistry, for example, to access triterpene natural products (FIG. 4d)[125,126]. These reactions and later oxidation of the sesquiterpene valencene[127,128] are among the few examples of K-S reactions that use the C—H substrate as the limiting reagent (FIG. 4j). Adaptation of K-S-type reactivity has led to oxidation of aliphatic C—H bonds. For example, di-*tert*-butyl peroxide (DTBP) has been used as an oxidant in combination with nitrogen-ligated Cu complexes to achieve *tert*-butyletherification of cyclohexane[129] and dehydrogenative coupling of carboxylic acids with cyclohexane[130]. These reactions use a large excess of the C—H substrate (≥ 10 equiv).

K-S-type reactions may be used to achieve C—N bond formation, for example, with amide, sulfonamide, and imide coupling partners (FIG. 4g-i)[118,131-136]. The reactions commonly use *tert*-butyl acylperoxides (i.e., derivatives of TBPB) or DTBP as the oxidant. For example, TBPB derivatives with electron-withdrawing groups on the benzoyl group (3-Cl, 3-CF_3) achieve C—N coupling between primary and secondary sulfonamides and simple methylarenes (25 equiv relative to the nitrogen nucleophile) (FIG. 4h)[133]. A well-defined diketiminate-ligated Cu complex was used in combination with DTBP to support amination of a small number of aliphatic C—H substrates (indane, ethylbenzene, cyclohexane) with 1-adamantylamine and other aliphatic amines (FIG. 4g)[134]. The amine ligand undergoes exchange with a [Cu]—O*t*Bu intermediate to form a copper(II)-amido complex, and mechanistic studies indicate that this species can promote direct HAT from the C—H substrate. This reactivity differs from most K-S-type reactions, which feature HAT by an alkoxyl radical. Amination of cyclic and acyclic aliphatic C—H bonds proceeds with various amides, sulfonamides, and phthalimide using a 4,7-dimethoxyphenantronline/CuI catalyst with DTBP as the oxidant (FIG. 4i)[135]. A variant of the conventional K-S mechanism was proposed, in which a Cu^{I}-amidate activates the peroxide to generate the *t*BuO•, which promotes HAT from the C—H substrate[135]. The resulting alkyl radical reacts with a Cu^{II}-amidate species to afford the C—N bond. A photochemical copper(II)-catalyzed method initiates O—O bond homolysis of DTBP at room temperature, supporting C—N coupling of alkanes with various nitrogen nucleophiles under mild conditions[136]. As with the other K-S-type reactions involving aliphatic substrates, a large excess of the C—H substrate (≥ 10 equiv) is used in these reactions.

K-S reactivity may be used to support C—C coupling reactions with various carbon nucleophiles, including 1,3-dicarbonyl compounds, arylboronic esters, and fluorinated arenes. In the reaction of benzylic C—H substrates with TBPB as the oxidant, C—C coupling with 1,3-dicarbonyl compounds proceeds via sequential formation of a benzylic benzoate, followed by nucleophilic displacement of the benzoate (FIG. 4f)[137]. Redox-neutral alkyenylation of C—H bonds adjacent to oxygen in THF (and related cyclic ether solvents) exhibits feature reminiscent of K-S reactions, employing terminal alkynes as coupling partners together with *t*BuOOH and catalytic $Cu^{I}Cl$ under blue LED irradiation[138]. Arylation of benzylic C—H bonds with arylboronic esters proceeds with DTBP as the oxidant (FIG. 4k)[139]. The reaction is proposed to involve transmetalation between the arylboronic ester and a Cu^{II}–O*t*Bu intermediate to afford an arylcopper(II) intermediate, which undergoes coupling with a benzylic radical generated by HAT from *t*BuO•. This reaction affords a variety of diarylmethane and diarylalkane products. β-Diketiminate copper catalysts support direct C—H/C—H coupling of polyfluoroarenes and allylic, benzylic, and aliphatic C—H substrates using DTBP as the oxidant (FIG. 4l)[140]. Each of these reactions employs the C(sp^3)—H substrate in excess (e.g., 10 equiv) relative to the coupling partner; however, they have synthetic appeal beyond the related C—O and C—N coupling reactions because the more valuable coupling partner (alkyne, arylboronic acid, fluoroarene) is used as the limiting reagent. Thus, inexpensive cyclic ethers and alkylarenes may be used to support alkylation of valuable coupling partners.

Copper/NFSI-catalyzed radical-relay reactions

The need for excess C—H substrate restricts the synthetic utility of K-S and related oxidative coupling reactions; however, this limitation has been overcome by using NFSI, rather than peroxide-based oxidants, in combination with copper catalysts. These methods show very high selectivity for benzylic C(sp^3)—H bonds relative to other positions (e.g., 3° C—H bonds), and they are among the most versatile methods for site-selective C—H functionalization and cross-coupling, leading to the formation of new C—X (X = halide, psueudohalide), C—N, C—O, C—S, and C—C bonds (FIG. 5).

Cu/NFSI-catalyzed C(sp^3)—H functionalization and functionalization/diversification methods.

The first Cu/NFSI benzylic C—H functionalization method led to sulfonimidation of benzylic C—H bonds, using NFSI as the HAT reagent and as the coupling partner (FIG. 5a)[141]. This method, which is compatible with primary and secondary benzylic C—H bonds, highlighted the use of the benzylic C—H substrates as the limiting reagent. The first demonstration of Cu/NFSI reactivity for oxidative coupling of C—H substrates and a separate nucleophilic reaction partner featured cyanation of benzylic C—H bonds with TMSCN (TMS = trimethylsilyl) (FIG. 5b)[142]. These reactions employ a chiral bisoxazoline ligand and achieve high enantioselectivity (many with >90% ee), good functional group compatibility, and very high site selectivity for less hindered secondary benzylic C—H bonds. Density functional theory (DFT) calculations suggest enantioselective C—C bond formation arises from reversible radical addition to a chiral Cu^{II}–CN species followed by selectivity determining reductive elimination (FIG. 6a, inner sphere radical coupling).

Benzylic C—H trifluoromethylation was demonstrated using a copper(I) source, NFSI or Selectfluor II as the oxidant, and (bpy)$Zn(CF_3)_2$ as the trifluoromethyl nucleophile (FIG. 5c)[143]. NFSI is generally the most effective oxidant for primary benzylic substrates, but Selectfluor II, which generates a more reactive nitrogen-centered radical, exhibits improved reactivity with electron-deficient substrates. Improved outcomes were observed with secondary benzylic substrates when using $Zn(OTf)_2$ and $Zn(OAc)_2$ additives, an effect attributed to more efficient transmetalation of the trifluoromethyl anion to copper(II) and higher concentration of Cu^{II}–CF_3 species.

Cu/NFSI-catalyzed C—H azidation is achieved by using trimethylsilyl azide ($TMSN_3$) as the nucleophilic coupling partner (FIG. 5d)[144]. The reaction exhibits very high site-selectivity for secondary benzylic C—H bonds over tertiary aliphatic and benzylic C—H bonds. This selectivity, which exceeds that observed with other radical azidation methods[66, 145, 146] is rationalized by the steric and electronic properties of the sulfonimidyl *N*-centered radical that promotes HAT. Azide is an effective ammonia surrogate, in addition to serving as a precursor to various heterocycles (FIG. 5d). Complementary Cu/NFSI methods have been developed for coupling with other ammonia surrogates, including carbamates[147], sulfonamides, and primary carboxamides (FIG. 5e)[148]. These and several other Cu/NFSI-catalyzed oxidative coupling reactions afford racemic products, even when using chiral bisoxazoline ligands similar to those in the cyanation reaction[144]. Experimental and computational data indicate the azidation reaction proceeds via a radical-polar crossover

mechanism in which the benzylic radical is oxidized to a cation prior to reaction with an azide nucleophile. The different stereochemical outcomes of these reactions is likely correlated with the influence of different nucleophiles as ligands that modulate the redox properties of the Cu^{II} species, altering the fate of the radical intermediate.

TMSNCS and TMSNCO are additional effective pseudohalide coupling partners, affording benzylic thiocyanate and isocyanate derivatives (FIG. 5f and 5g)[149,150]. Inter- and intramolecular competition studies in the thiocyanation reaction indicate that HAT from benzylic C—H bonds favors 3° > 2° > 1° positions, differing from the azidation reaction, which favors 2° sites. These observations suggest the identity of the HAT reagent may not be identical in all reactions. Both thiocyanate and isocyanate product classes represent versatile precursors to other valuable products. The benzylic thiocyanate products may be converted in two- or three-step sequences, without isolation of the intermediates, into other products, including isothiocyanates, thioureas, trifluoromethylthio, difluoromethylthio, 5-*S*-benzbromarone-linked tetrazole, and disulfide derivatives. This concept was expanded for benzylic isocyanates through the development of a benzylic isocyanation/amine coupling sequence suitable for implementation in a high-throughput format, enabling efficient access to large numbers of benzylic ureas with drug-like physiochemical properties[150].

The C—H functionalization/diversification strategy illustrated for azides, thiocyanates, and isocyanates in FIGS. 5d, 5f, and 5g, is even more versatile with C—H halogenation methods. C—H fluorination was demonstrated by variation of the original Cu/NFSI conditions, which led to C—H sulfonimidation (FIG. 5h)[31,151]. The use of a Brønsted base (Li_2CO_3) and $MeB(OH)_2$ as an in situ reductant for the copper catalyst (i.e., a "redox buffer"; see mechanistic discussion below) account for the switch in selectivity[31] via initiation of a Cu^{I}-promoted radical-chain pathway involving NFSI (see Radical Chain section above for further discussion and additional references). From a synthetic perspective, benzyl fluorides are not inert like many other alkyl fluorides but are quite labile. This feature may be exploited to support nucleophilic displacement of the fluoride, promoted by the presence of a hydrogen-bond donor, such as hexafluoroisopropanol (HFIP), or a Lewis acid, such as boron trifluoride diethyl etherate (BF_3•Et_2O)[152-155]. The resulting fluorination/substitution sequence enables the replacement of benzylic C—H bonds with a wide range of oxygen-, nitrogen-, and carbon-based groups[151]. Similar concepts have been demonstrated with a Cu/NFSI-catalyzed chlorination method (FIG. 5i), in which chlorination/substitution access products that can be difficult to access under the acidic conditions required for fluoride substitution[156]. For example, reactions of phenols with benzyl fluorides promoted by HFIP leads to C—C bond formation, with phenol reacting at the ortho position, while reactions with benzyl chlorides under basic conditions leads to C—O bond formation, with phenol reacting at the oxygen atom. These two-step functionalization/diversification methods, initiated by fluorination and chlorination, enable net C—H functionalization with oxidatively sensitive nucleophiles that would not be compatible with a one-step oxidative coupling method using NFSI as the oxidant. This reactivity complements an independent Cu-catalyzed chlorination approach using a dichloramine-T as the oxidant that selectively functionalizes $C(sp^3)$—H bonds in ketones, enones, and alkylbenzenes[157,158]. This study also demonstrated nucleophilic displacement of secondary benzyl chlorides with *N*-Bocpiperazine, demonstrating another example functionalization/diversification.

Variants of NFSI have been developed in which one phenylsulfonyl group in NFSI is replaced with a *tert*-alkyl group and the other phenysulfonyl is replaced an electron-deficient arylsulfonyl (e.g., 4-CF_3- or 3,5-$(CF_3)_2$-phenyl). These reagents have been used to achieve complementary radical-relay C—H functionalization, including regio- and enantioselective cyanation of allylic C(sp^3)—H bonds with TMSCN (with limiting C—H substrate)[159], and thiolation of C—H bonds with *S*-aryl benzenethiosulfonates (3 equiv C—H substrate) (see FIG. 3Cb)[84]. In the former study, DFT calculations implicate a Cu^{II}-bound nitrogen-centered radical as the reactive HAT species, and this species was proposed to account for modulation of site selectivity. This proposal aligns with the observations above that the specific HAT species could be modified under different conditions. Selectfluor is a related N—F reagent that generates an amine radical-cation, which is a stronger HAT reagent than the *N*-centered radical derived from NFSI. In presence of copper catalysts, Selectfluor enables HAT with aliphatic C—H substrates, used in excess (3 equiv to solvent level) relative to the coupling partner[160]. Esterification was achieved with various carboxylic acids as coupling partners in presence of pentanenitrile as additive[160]. The Ritter-type amidation product derive from pentanenitrile was obtained when triflic acid was attempted as the coupling partner (i.e., in an effort to use triflate as the nucleophile).

Cu/NFSI-catalyzed C(sp^3)—H cross coupling.

Cross-coupling methods that combine reagents from diverse pools of substrates are especially important methods in synthetic chemistry, and several examples of C—H cross coupling have been achieved by using Cu/NFSI catalysis. The coupling of benzylic C—H substrates and alcohols enable access to a diverse scope of benzyl ethers (FIG. 5j)[161]. Medicinally relevant benzylic C—H substrates undergo cross coupled with sterically and electronically diverse aliphatic alcohols. Mechanistic studies indicate that this reactivity proceeds by a radical-polar crossover mechanism (FIG. 6b). In addition, successful reactivity required inclusion of a dialkyl phosphite additive as a sacrificial reductant to regenerate the reduced catalyst (see mechanistic discussion below). Azoles have also been used as reaction partners in Cu/NFSI-catalyzed benzylic C—H cross-coupling reactions. Pyrazoles exhibit controlled regioselectivity, with different N-site coupling observed when the reaction was conducted in the presence of a tetrabutylammonium halide (TBAX) or silyl triflate additive (FIG. 5k)[162]. The kinetically favored N^2 site selectivity with TBACl as the additive contrasts the N^1 site selectivity more commonly observed, for example, in substitution reactions with pyrazolide reagents[163, 164]. Various azoles and other nitrogen heterocycles are effective coupling partners.

Cu/NFSI-catalyzed methods enable carbon-carbon bond formation via benzylic C—H cross-coupling with aryl and alkynyl nucleophiles. While K-S-type oxidative coupling of benzylic substrates and aryl boronic acids with DTBP as the oxidant uses excess C—H substrate[139], the use of NFSI as the oxidant enables reactions to proceed with limiting C—H substrate[165]. The latter reactions are effective with electron-deficient arylboronic acids and proceed at ambient temperature, rather than the high temperatures (90 °C) required for K-S-type reaction. Use of a chiral bisoxazoline ligand supports enantioselective arylation of benzylic C—H bonds of alkylnaphthalenes and related derivatives (FIG. 5l)[166]. Enantioselective coupling of benzylic C—H bonds and alkynyl silane derivatives is also possible, again using

chiral bisoxazoline ligands (FIG. 5m)[167]. A modified N—F reagent, in which the two phenyl groups of NSFI were replaced with a 4-fluorophenyl and a 1-naphthyl substituent aryl, led to improvements in the yield and enantioselectivity. The alkylarene is used as the limiting reagent in combination with simple alkynyl trimethoxylsilane derivatives.

Mechanistic features of Cu/NFSI-catalyzed C—H functionalization and cross-coupling methods.

The catalytic cycle for these Cu/NFSI reactions is believed to follow a mechanism similar to that proposed for K-S reactions (FIG. 6)[142]. Reductive activation of NFSI by copper(I) initiates the reaction, generating a Cu^{II}–F intermediate and a nitrogen-centered radical (•NSI). The latter species promotes HAT from the C—H bond to generate a diffusible benzylic radical. Studies of a closely related allylic cyanation reaction, which employed modified N—F reagents, provided evidence for an adduct between Cu^{II} and the *N*-centered radical as the HAT reagent[159]. Modification of the nitrogen-centered radical in this manner could account for some variations in site selectivity that have been observed in different Cu/NFSI described above.

Functionalization of the organic radical can proceed by several different pathways. In some reactions, the nucleophilic coupling partner (e.g., TMSCN) exchanges with fluoride to generate a Cu^{II}–Nuc species. Subsequent addition of the benzylic radical to the Cu^{II} center affords an Cu^{III}(benzyl)(Nuc) intermediate that can undergo reductive elimination to afford the desired coupling product via an inner-sphere mechanism (FIG. 6a). This pathway rationalizes the enantioselective outcomes of certain coupling reactions, including benzylic cyanation, arylation, and alkynylation. Computational studies of the cyanation reaction suggest radical addition to Cu^{II} is reversible and stereoselectivity is determined in the reductive elimination step[142]. Alternatively, radical functionalization can proceed via a radical-polar crossover pathway (FIG. 6b, radical-polar crossover), involving outer-sphere electron transfer from the radical to Cu^{II}. The resulting benzyl cation is then trapped by a nucleophile to afford the desired product. This pathway is supported by racemic product formation in many of the reactions in FIG. 5, such as etherification[161], which has also been analyzed by DFT computational studies. DFT analysis of the azidation reaction indicated that radical addition the distal nitrogen of a coordinated azide ligand (FIG. 6c) is energetically similar to the radical-polar crossover mechanism[144]. As noted above, the electronic/donor properties of different nucleophiles are expected to influence the $Cu^{II/I}$ redox potential and influence whether a benzyl radical adds to Cu^{II} to generate a Cu^{III} intermediate, introducing the possibility of enantioselective bond formation, or it undergoes outer-sphere electron transfer, resulting in racemic product formation.

The •NSI species generated by reductive activation of NFSI by Cu^{I} can oxidize a second equivalent of Cu^{I} to generate a Cu^{II}–NSI species, rather than promoting HAT from the C—H substrate (FIG. 6, bottom cycle). This undesired side reaction leads to unproductive consumption of the NFSI oxidant and Cu^{I} species, stalling the reaction. This problem was first identified in the study of benzylic etherification[161], and it was overcome by identifying dialkylphosphite as a mild reductant that slowly reduces Cu^{II} to Cu^{I} during the reaction, without undergoing direct reaction with NFSI. This "redox buffer"

concept has been employed in a number of Cu/NFSI radical-relay reactions, including etherification[161], isocyanation[150], fluorination[31], chlorination[156], and azole coupling[162]. Reagents that have been used as redox buffers include dialkylphosphites[150,156,161,162], $MeB(OH)_2$, and B_2pin_2[31,151]. Not all Cu/NFSI radical-relay reactions require a redox buffer. If the coupling partner, such as TMSCN or $ArB(OH)_2$ in the cyanation and arylation reactions, can undergo background reduction of Cu^{II}, for example, via homocoupling to generate cyanogen or biaryls, then no redox buffer is required.

Radical-relay oxidative coupling reactions with catalysts other than copper

Various metals other than copper have been used to support synthetically useful oxidative coupling reactions that proceed via radical intermediates (FIG. 7). Iron(II) chloride and DTBP support the cross coupling of benzylic C—H bonds and 1,3-dicarbonyl compounds[168] and imidazoles[169] (FIG. 7, Fe), and iron(III) chloride and DTBP was used to achieve coupling of 2-benzylbenzoxazoles and anilines[170]. Iron(II) acetate with nitrogen donor ligands catalyzes azidation of various $C(sp^3)$—H bonds with a hypervalent azidoiodine(III) reagent[145], often favoring tertiary C—H functionalization. This reactivity was applied to late-stage functionalization of various complex molecules[171]. Cobalt(II) bromide catalysts support cross-coupling of benzylic C—H bonds with amides and sulfonamides and with DTBP as oxidant (FIG. 7, Co)[172]. Two equivalents of the C—H substrate were used in these reactions. A radical-polar crossover pathway involving a benzylic cation was proposed.

Nickel catalysts have been paired with peroxide oxidants to support oxidative alkynylation, arylation, and methylation of $C(sp^3)$—H bonds. A Ni/Cu/Ag-cocatalyst system promotes oxidative $C(sp^3)$—H alkynylation of unactivated alkanes (as a cosolvent), using terminal alkynes as the limiting reagent (FIG. 7, Ni)[173]. Ni/triphenylphosphine catalyst systems promote arylation of aliphatic $C(sp^3)$—H bonds with arylboronic acids coupling partners as the limiting reagent[174,175]. Effective C—H substrates include tetrahydrofuran (THF), 1,4-dioxane, and cyclohexane, which are used as the solvent in the reactions. Methylation of $C(sp^3)$—H bonds with limiting C—H substrates is enabled by photosensitization of peroxides and nickel-mediated radical coupling (FIG. 7, Ni)[176]. Tertiary alkoxyl radicals generated from O—O homolysis of peroxides undergo HAT with C—H substrates and self-decomposition β-methyl scission to produce methyl radicals. Various reaction parameters, including temperature, concentration, solvent, and structures of peroxides, may be tuned to balance the relative rates of HAT and methyl-radical formation. Protonation of C—H substrates containing basic amines deactivates $C(sp^3)$—H sites adjacent to nitrogen to enable methylation at the benzylic positions. This methylation method creates opportunities to explore “magic methyl” effects on medicinally relevant building blocks and drug molecules[177].

Silver catalysts have also been used in radical reaction reactions (FIG. 7, Ag)[178]. A silver-promoted oxidative benzylic C—H trifluoromethoxylation with C—H substrate as the limiting reagent uses potassium persulfate as oxidant[179]. The reaction favors functionalization at secondary > primary > tertiary benzylic C—H site and can be modified to introduce a fluorine atom and a trifluoromethoxy group at the same site.

Photochemical radical-relay reactions

Photochemical and visible-light photoredox methods provide a versatile strategy to generate organic radicals from a C(sp^3)—H substrate and promote radical-relay coupling with diverse functional groups[180-186]. The reactions are initiated by abstraction of a hydrogen atom from the C—H substrate. The HAT reagent is generated by photocatalyst-mediated activation of an oxidant, such as a hypervalent iodine reagent, *N*-acyloxyphthalimide, or persulfate, or by direct photoactivation of a reagent, such as decatungstate or benzophenone (FIG. 8)[187]. The introduction of functional groups, including hydroxyl, ammonia surrogates, trifluoromethyl, alkyl, and aryl groups, can take place by various mechanisms, similar to the methods outlined above (cf. FIG. 1Cb and FIG. 6). Radical-polar crossover reactions, which generate the corresponding cation or anion (FIG. 8a, SET), are used to support subsequent coupling reactions with nucleophiles and electrophiles, respectively. Transition-metal reagents and cocatalysts can promote coupling via radical-polar crossover or inner-sphere coupling pathways (FIG. 8a, Cu, Ni). Iodine has been used to trap and support further functionalization of the alkyl radicals (FIG. 8a, I). Examples of these photochemical radical-relay reactions will be surveyed below, divided into C(sp^3)—H functionalization (one-for-one replacement of a C—H bond with another functional group) and cross-coupling reactions (reaction of a C—H bond with a group of similar reagents).

Photoredox C(sp^3)—H functionalization reactions.

Photoredox-promoted radical-relay methods have been used to support functionalization of C(sp^3)—H bonds with halogens, pseudohalogens, acetate, ammonia surrogates, and a trifluoromethyl group. Nucleophilic fluorination of C(sp^3)—H bonds has been achieved in two complementary studies by using Ir-based photoredox catalysts. In one case, single electron transfer (SET) from the excited state photocatalyst promotes reductive activation of *N*-acetoxyphthalimide[188]. N—O cleavage and decarboxylation of the acetoxyl radical generates a methyl radical that promotes HAT from a benzylic or allylic C—H bond. The stabilized carbon-centered radical then undergoes SET oxidation by the Ir^{IV} photocatalyst to generate a carbocation that can react with $Et_3N{\bullet}HF$. A related study employed a peroxide-based oxidant (TBPB) with an Ir photoredox catalyst, resulting in generation of *tert*-butoxyl radical, which promotes HAT from secondary/tertiary benzylic C—H bonds[189]. A similar radical-polar crossover step, involving SET oxidation of the radical by Ir^{IV}, generates a carbocation that reacts with $Et_3N{\bullet}HF$. Both studies prioritized fluorination; however, other nucleophiles were shown to trap the carbocation under the reaction conditions, including chloride, azide, alcohols, thiols, and 1,3,5-trimethoxybenzene (FIG. 9a, SET).

C(sp^3)—H oxygenation and amidation has been achieved by pairing photoredox catalysts with hypervalent iodine oxidants. $[Ru(bpy)_3]Cl_2$ mediates photochemical reduction of benziodoxole (BI—OH) and its perfluorinated analog (PFBI—OH) to generate species that promote HAT from tertiary aliphatic and benzylic C(sp^3)—H bonds. The Ru^{III} state of the photocatalyst then promotes SET oxidation of the organic radical to generate a carbocation, which can react with H_2O to afford the hydroxylation product[190]. Inclusion of CH_3CN or PhCN in the reaction mixtures accesses the corresponding acetamide or benzamide products via a Ritter-type mechanism (FIG. 9a, SET)[191,192]. Acetoxylation of primary and

secondary benzylic C—H bonds proceeds with and acridinium-based photocatalyst and phenyliodonium diacetate (PIDA) as the oxidant and source of acetate[193]. Photoredox-based reductive activation of PIDA is proposed to generate a methyl radical, which undergoes HAT with the C—H substrate. The oxidized photocatalyst can then oxidize the organic radical to a carbocation intermediate, and subsequent reaction of acetate with the carbocation affords the acetoxylated product.

An alternative approach for functionalization of organic radicals involves SET reduction to carbanions, followed by reaction with different electrophiles (FIG. 9a, SET)[194,195]. This approach has been used to convert alkylarenes to aryl acetic acids and related products via C—H coupling with CO_2[194] and to homobenzylic secondary and tertiary alcohols via C—H coupling with aldehydes and ketones[195]. These reactions use carbazole- or diarylamine-substituted dicyanoarene photocatalysts. The excited-state photocatalyst oxidizes the thiolate of iPr$_3$SiSH to generate a thiyl radical, which promotes HAT from the activated C—H bond. The reduced photocatalyst then promotes SET reduction of the carbon-centered radical to afford a carbanion that can react with an electrophile (CO_2 or a ketone) to form a C—C bond.

Light-assisted iodine-catalyzed intramolecular C(sp^3)—H amination been the focus of considerable development[25] Intermolecular amination of C(sp^3)—H bonds has been achieved using bis(4-bromobenzoyloxy)iodobenzene as oxidant and trifluoromethanesulfonamide (H_2NTf) as an HAT reagent and ammonia surrogate (FIG. 9d, I)[196]. In situ reaction of H2NTf and the hypervalent iodine reagent generates *N*-iodo triflamide (I–NHTf), which can undergo light-induced homolysis of the N—I bond to afford a sulfonamidyl radical. This step is followed by HAT from the C(sp^3)—H substrate, carbon—iodine bond formation, and nucleophilic substitution of the iodide to form the C—N product.

Installation of trifluoromethyl group has also been achieved via a photoredox radical-relay approach with cooperative copper catalysis (FIG. 9, Cu). The CF_3 group was introduced to the benzylic sites by irradiating a reaction mixture of ammonium persulfate and a bench-stable bpyCu(CF_3)$_3$ complex[197] in mixed organic/aqueous media (acetone/H_2O 1:1) (FIG. 9b, Cu)[198]. This strategy was also applied to trifluoromethylation of unactivated C(sp^3)—H bonds[199]. HAT from C—H substrates could be promoted by sulfate radical anion or trifluoromethyl-based radical, via light-induced homolysis of persulfate or bpyCu(CF_3)$_3$, respectively. The organic radical then reacts with an equivalent of the Cu—CF_3 species to afford a trifluoromethylated product. C(sp^3)—H trifluoromethylation has also been achieved using bpyCu(CF_3)$_3$ and oxone[200]. In this case, the mechanism is proposed to involve HAT from the C—H substrate by a trifluoromethyl radical, oxidation of the carbon-centered radical to a carbocation by oxone, and reaction of an anionic trifluoromethyl source with the carbocation. In yet another approach, sodium decatungstate has been used in combination with a copper catalyst ($CuCl_2$) and a trifluoromethyl hypervalent iodine-based oxidant to convert C(sp^3)—H bonds to the corresponding C(sp^3)—CF3 products (FIG. 9b, Cu)[201]. The photoexcited decatungstate promotes HAT to form a carbon-centered radical, and a Cu^{II}—CF_3 species, generated in situ from $CuCl_2$ and the CF_3 source, is proposed to react with the organic radical to afford the trifluoromethylated products.

Photoredox C(sp^3)—H cross coupling.

Photoredox methods enable cross coupling of benzylic and aliphatic C—H substrates with diverse aryl or alkyl halide reaction partners. Three general strategies have been employed to support HAT in these reactions: (a) combining a photocatalyst with a tertiary amine to generate an amine radical cation species, (b) use of a reagent that is capable to promoting HAT from its photoexcited state, and (c) photochemical activation of a nickel halide to generate a halogen radical HAT species.

The first example of this reactivity used 3-acetoxyquinuclidine, an Ir-based photocatalyst, and nickel(II) bromide to support cross coupling of activated C(sp^3)—H bonds, such as those adjacent to nitrogen in pyrrolidines, with aryl bromides/chlorides (FIG.9c, Ni)[202]. SET oxidation of 3-acetoxyquinuclidine by the excited-state Ir^{III} photocatalyst generates a quinuclidine radical cation capable of promoting HAT from the C(sp^3)—H bond. This radical generation process is paired with a Ni-based radical functionalization cycle. The nickel co-catalyst reacts with the organic halide species to afford an organonickel(II) species, which promotes C—C coupling by reaction with the radical derived from the C—H substrate. Cross coupling of activated C(sp^3)—H and alkyl halides employing quinuclidine, an Ir-based photoredox catalyst, and nickel(II) bromide has been achieved via similar mechanistic pathway[203]. Quinuclidine also promotes HAT from aldehyde[204] and the α-C—H bonds of alcohols[205] to enable direct arylation and alkylation via Ni-catalyzed cross coupling. Nitrogen-centered radicals from sulfonamides have been shown to abstract hydrogen atoms from C—H bonds adjacent to heteroatoms, generating radicals that undergo Ni-catalyzed cross coupling with alkyl halides to afford alkylated products[206]. Photoexcited 4CzIPN (1,2,3,5-tetrakis(carbazol-9-yl)-4,6-dicyanobenzene) is proposed to oxidize sulfonamide anion to the nitrogen-centered radical, which is responsible for HAT.

TBADT serves as a combined photocatalyst/HAT reagent and supports arylation of strong aliphatic C—H bonds with aryl bromides[207]. Disproportionation of two singly reduced decatungstate species regenerates the active HAT photocatalyst and the doubly reduced decatungstate species, which can reduce the nickel cocatalyst as needed for activation of the aryl bromide coupling partner. Benzophenone derivatives are similar to TBADT in their ability to promote HAT from their photoexcited triplet state[208,209]. This feature has been exploited in combination with nickel catalysis for cross coupling of activated C(sp^3)—H bonds with aryl and alkyl halides (FIG. 9c, Ni)[210]. 4,4'-Dichlorobenzophenone (FIG. 8b, Ketone-**2**) has been used as a photocatalyst to achieve arylation of primary benzylic C(sp^3)—H bonds[211]. Aryl halides, including chlorides, bromides, and iodides, can be utilized as coupling partners. Benzaldehyde has also been used as a photocatalyst for arylation and alkylation of activated C(sp^3)—H bonds (FIG. 9c, Ni)[212,213].

Arylation of activated C(sp^3)—H bonds has been achieved by combining an Ir-based photoredox catalyst and Ni cocatalyst, in the absence of an HAT reagent (FIG. 10Ba). In the coupling of aryl bromides with THF and other solvents with activated C—H bonds, the excited-state photocatalyst Ir^{III}* is proposed to undergo triplet-triplet energy transfer with a $ArNi^{II}$–Br species to generate a triplet Ni^{II}* species. (FIG. 10Aa). HAT from the C(sp^3)—H bond may involve a bromine radical or proceed via a concerted

four-membered transition state involving the Ni—Br bond. The resulting carbon-centered radical can react at Ni to afford the C(sp^3)—C(sp^2) bond [214]. A complementary study, involving the coupling of aryl chlorides with THF and related solvents (FIG. 10Bb) [215], proposes that the Ir^{III} photocatalyst serves as a SET reagent. Oxidation of an $ArNi^{II}$–Cl intermediate by the excited state photocatalyst Ir^{III}* generates a Ni^{III} species. Subsequent loss of a chlorine atom leads to HAT from the activated C(sp^3)—H bond of the solvent to afford an organic radical that can undergo coupling with the arylnickel(II) species (FIG. 10Ab). The synthetic utility of the latter reaction was demonstrated in a separate report in the cross coupling of (hetero)aryl chlorides with 1,3-dioxolane as the solvent[216]. The resulting cross-coupled products are readily converted to (hetero)aryl aldehydes following a mild acidic workup at room temperature. An enantioselective benzylic C—H arylation has been achieved with an Ir-based photocatalyst, nickel(II), and a chiral bis-imidazoline ligand (FIG. 10Bc)[217]. Aryl bromide coupling partners generate $ArNi^{II}$–Br, which is proposed to generate bromine radical as the HAT reagent upon irradiation in the presence of a photocatalyst. An enantioselective benzylic C(sp^3)—H alkenylation reaction has also been achieved with alkenyl bromides as the coupling partners in presence of an Ir-photoredox catalyst, nickel(II), and a chiral bis-imidazoline-based ligand[218]. Complementary nickel/photoredox dual catalysis enables acylation[219] and arylation[220] reactions of α-amino C(sp^3)—H bonds. In these cases, *N*-arylpyrrolidine substrates are proposed to generate stabilized α-amino radicals via a more conventional process involving SET oxidation of the substrate.

Electrochemical radical-relay reactions

Electrochemical methods provide additional strategies to achieve C(sp^3)—H functionalization via radical relay[221,222]. *N*-hydroxyphthalimide (NHPI) was first demonstrated as an electrochemical mediator for C(sp^3—H) oxygenation in the 1980s[223-225]. NHPI undergoes proton-coupled oxidation to phthalimide *N*-oxyl (PINO) as the electrode, and PINO- mediated HAT then generates an organic radical that can react with O_2 or other oxidants, resulting in C—H functionalization (FIG. 11Aa)[226]. These methods complement transition-metal/NHPI cocatalyst systems for C—H oxygenation with O_2[68,71,72]. Modified NHPI derivatives can lead to improved performance, evident from the use of tetrachloro-*N*-hydroxyphthalimide (Cl_4NHPI) as the HAT mediator in electrochemical oxidation of allylic C(sp^3)—H bonds (FIG. 11Ab) [227] , and an electrochemical NHPI/O_2 system proved effective for C—H oxygenation of alkyl-substituted heterocycles that exhibit poor reactivity with a chemical Co/NHPI/O_2 catalyst system (FIG. 11Ac)[71]. Flow conditions have been developed for the latter process[228].

Different mediators provide a means to expand reactivity beyond activated C—H bonds. Electrochemical oxidation of quinuclidine generates an amine radical cation that promotes HAT and oxygenation of diverse C(sp^3)—H bonds under aerobic conditions (FIG. 11Ad)[229]. *N*-alkyl ammonium ylides have been developed as a new class of electrochemical mediators for C(sp^3)—H oxygenation through the support of computational method (FIG. 11Ae)[230]. These reagents show modified chemo- and site-selectivity relative to previous chemical and electrochemical methods for C(sp^3)—H oxygenation.

NHPI has been paired with iodine, rather than O_2, to enable the iodination of methyl arenes[231]. The resulting benzyl iodide may be employed in subsequent S_N2-base derivatization reactions to access new C—C, C—O, and C—N bonds or undergo *in situ* substitution, for example, by pyridine (FIG. 11Af). This mediated HAT strategy allows electrochemical C—H functionalization to proceed at electrode potentials 0.7–1.3 V lower than those required by conventional SET-initiated electrochemical benzylic C—H functionalization methods[232,233].

Metal-oxo complexes capable of promoting C—H oxygenation have been generated via electrochemical proton-coupled oxidation of metal-aquo complexes (FIG. 11Ba). Electrochemical oxidation of $[(TAML)Fe^{III}(OH)_2]Na$ (TAML = tetraamido macrocyclic ligand) generates Fe^{IV} and Fe^{V} oxo species. The Fe^{V}-oxo is more reactive and oxidizes secondary benzylic C—H bonds to ketones using water as oxygen-atom source (FIG. 11Bb)[234]. Ruthenium-based oxo species derived from *cis*-bis(4,4'-di-*tert*-butylpyridine)ruthenium complex effects electrochemical hydroxylation of $C(sp^3)$—H bonds (FIG. 11Bc)[235]. Basic amines are tolerated, owing to the use of acidic reaction conditions that protect the amines as ammonium salts.

Two complementary electrochemical methods have been developed for $C(sp^3)$—H azidation. Manganese(III) porphyrin or salen complexes and sodium azide promote azidation of $C(sp^3)$—H bonds (FIG. 11C)[236]. The reaction is proposed to proceed via oxidation of Mn^{III} to a Mn^{IV}-diazide species, which promotes HAT from the substrate to generate an organic radical that affords an azide product via coupling with another Mn^{IV}-diazide complex. An electrophotochemical azidation protocol uses MnF_2 in combination with a ketone-based photocatalyst [e.g. 9-fluorenone, 2,3-dichloro-5,6-dicyano-p-benzoquinone (DDQ), bis(4-methoxyphenyl)methanone] and sodium azide (FIG. 11D)[237]. The excited-state photocatalyst promotes HAT, and an electrochemically generated Mn^{III}-azide is proposed to react with the carbon-centered radical.

Conclusion

Radical reaction pathways offer some of the most versatile methods available for $C(sp^3)$—H functionalization and cross-coupling, accessing synthetic scope and utility that is unmatched by other reaction pathways. Major advances have been made in each of the different radical reaction classes, including radical chain, radical rebound, and radical relay. Many of these reactions are able to use the C—H substrate as the limiting reagent, addressing one of the long-standing limitations of this field and supporting application to late-stage functionalization. Radical-relay methods are particularly versatile. These reactions not only enable installation of a specific functional groups, including -CN, —CF_3, —N_3, —OH, —SCN, —F, —Cl, —NCO, but also provide the basis for sequential functionalization/diversification methods and direct cross-coupling methods that leverage substrates derived from large pools of reaction partners, such as alcohols, amines/amides, arylboronic acids, and aryl halides. The latter feature greatly expands the scope of accessible products relative those obtained from typical C—H "functionalization" methods and has profound implications for drug discovery and medicinal chemistry where access to diverse structures is crucial to the success of the endeavors.

Acknowledgements

This work was supported by funding from the NIH (R35 GM134929).

References

1. He J, Wasa M, Chan KSL, Shao Q & Yu J-Q Palladium-catalyzed transformations of alkyl C—H bonds. Chem. Rev 117, 8754–8786 (2017). [PubMed: 28697604]
2. Jazzar R, Hitce J, Renaudat A, Sofack-Kreutzer J & Baudoin O Functionalization of organic molecules by transition-metal-catalyzed C(sp^3)—H activation. Chem. Eur. J 16, 2654–2672 (2010). [PubMed: 20143359]
3. Saint-Denis TG, Zhu R-Y, Chen G, Wu Q-F & Yu J-Q Enantioselective C(sp^3)—H bond activation by chiral transition metal catalysts. Science 359, eaao4798 (2018). [PubMed: 29449462]
4. Gupta A, Kumar J, Rahaman A, Singh AK & Bhadra S Functionalization of C(sp^3)—H bonds adjacent to heterocycles catalyzed by earth abundant transition metals. Tetrahedron 98, 132415 (2021).
5. Davies HML & Manning JR Catalytic C—H functionalization by metal carbenoid and nitrenoid insertion. Nature 451, 417–424 (2008). [PubMed: 18216847]
6. Doyle MP, Duffy R, Ratnikov M & Zhou L Catalytic carbene insertion into C—H bonds. Chem. Rev 110, 704–724 (2010). [PubMed: 19785457]
7. Roizen J, Harvey ME & Du Bois J Metal-catalyzed nitrogen-atom transfer methods for the oxidant of aliphatic C—H bonds. Acc. Chem. Res 45, 911–922 (2012). [PubMed: 22546004]
8. Yi H et al. Recent advances in radical C—H activation/radical cross-coupling. Chem. Rev 117, 9016–9085 (2017). [PubMed: 28639787]
9. Zhang C, Li Z-L, Gu Q-S & Liu X-Y Catalytic enantioselective C(sp^3)—H functionalization involving radical intermediates. Nat. Commun 12, 475 (2021). [PubMed: 33473126]
10. Studer A & Curran DP Catalysis of radical reactions: A radical chemistry perspective. Angew. Chem. Int. Ed 55, 58–102 (2016).
11. Labinger JA & Bercaw JE Understanding and exploiting C—H bond activation. Nature 417, 507–514 (2002). [PubMed: 12037558]
12. Sheldon RA & Kochi JK in Metal-catalyzed oxidations of organic compounds: Mechanistic principles and synthetic methodology including biochemical processes (Academic Press, Inc., New York, 1981).
13. Hermans I, Spier ES, Neuenschwander U, Turrà N & Baiker A Selective oxidation catalysis: Opportunities and challenges. Top. Catal 52, 1162–1174 (2009).
14. Quinn RK et al. Site-selective aliphatic C—H chlorination using *N*-chloroamides enables a synthesis of chlorolissoclimide. J. Am. Chem. Soc 138, 696–702 (2016). [PubMed: 26694767]
15. Schmidt VA, Quinn RK, Brusoe AT & Alexanian EJ Site-selective aliphatic C—H bromination using *N*-bromoamides and visible light. J. Am. Chem. Soc 136, 14389–14392 (2014). [PubMed: 25232995]
16. Czaplyski WL, Na CG & Alexanian EJ C—H Xanthylation: A synthetic platform for alkane functionalization. J. Am. Chem. Soc 138, 13854–13857 (2016). [PubMed: 27739673]
17. Tanwar L, Börgel J & Ritter T Synthesis of benzylic alcohols by C—H oxidation. J. Am. Chem. Soc 141, 17983–17988 (2019). [PubMed: 31689095]
18. Huang X & Groves JT Beyond ferryl-mediated hydroxylation: 40 years of rebound mechanism and C—H activation. J. Biol. Inorg. Chem 22, 185–207 (2017). [PubMed: 27909920]
19. Huang X & Groves JT Taming azide radicals for catalytic C—H azidation. ACS Catal. 6, 751–759 (2016).
20. Clark JR, Feng K, Sookezian A & White MC Manganese-catalysed benzylic C(sp^3)—H amination for late-stage functionalization. Nature Chem. 10, 583–591 (2018). [PubMed: 29713037]
21. Lovering F, Bikker J & Humblet C Escape from flatland: Increasing saturation as an approach to improving clinical success. J. Med. Chem 52, 6752–6756 (2009). [PubMed: 19827778]

22. Blakemore DC et al. Organic synthesis provides opportunities to transform drug discovery. Nature Chem. 10, 383–394 (2018). [PubMed: 29568051]
23. Guillemard L, Kaplaneris N, Ackermann L & Johansson MJ Late-stage C—H functionalization offers new opportunities in drug discovery. Nat. Rev. Chem 5, 522–545(2021).
24. Wolff ME Cyclization of N-halogenated amines (the Hofmann-Löffler reaction). Chem. Rev 63, 55–64 (1963).
25. Statement LM, Nakafuku KM & Nagib DA Remote C—H functionalization via selective hydrogen atom transfer. Synthesis 50, 1569–1586 (2018). [PubMed: 29755145]
26. Sarkar S Cheung KPS & Gevorgyan V C—H functionalization reactions enabled by hydrogen atom transfer to carbon-centered radicals. Chem. Sci 11, 12974–12993 (2020). [PubMed: 34123240]
27. Nodwell MB et al. Direct photocatalytic fluorination of benzylic C—H bonds with *N*-fluorobenzenesulfonimide. Chem. Commun 51, 11783–11786 (2015).
28. Pitts CR, Ling B, Woltornist R, Liu R & Lectka T Triethylborane-initiated radical chain fluorination: A synthetic method derived from mechanistic insight. J. Org. Chem 79, 8895–8899 (2014). [PubMed: 25137438]
29. Pitts CR et al. Direct, catalytic monofluorination of sp^3 C—H bonds: A radical-based mechanism with ionic selectivity. J. Am. Chem. Soc 136, 9780–9791 (2014). [PubMed: 24943675]
30. Bloom S et al. Iron(II)-catalyzed benzylic fluorination. Org. Lett 15, 1722–1724 (2013). [PubMed: 23527764]
31. Buss JA, Vasilopoulos A, Golden DL & Stahl SS Copper-catalyzed functionalization of benzylic C—H bonds with *N*-fluorobenzenesulfonimide: Switch from C—N to C—F bond formation promoted by a redox buffer and Brønsted base. Org. Lett 22, 5749–5752 (2020). [PubMed: 32790419]
32. Bloom S et al. A polycomponent metal-catalyzed aliphatic, allylic, and benzylic fluorination. Angew. Chem. Int. Ed 51, 10580–10583 (2012).
33. Xia J-B, Zhu C & Chen C Visible light-promoted metal-free C—H activation: Diarylketone-catalyzed selective benzylic mono- and difluorination. J. Am. Chem. Soc 135, 17494–17500 (2013). [PubMed: 24180320]
34. Halperin SD, Fan H, Chang S, Martin RE & Britton R A convenient photocatalytic fluorination of unactivated C—H bonds. Angew. Chem. Int. Ed 53, 4690–4693 (2014).
35. Bloom S, McCann M & Lectka T Photocatalyzed benzylic fluorination: Shedding “light” on the involvement of electron transfer. Org. Lett 16, 6338–6341 (2014). [PubMed: 25493423]
36. Carestia AM, Ravelli D & Alexanian EJ Reagent-dictated site selectivity in intermolecular aliphatic C—H functionalizations using nitrogen-centered radicals. Chem. Sci 9, 5360–5365 (2018). [PubMed: 30009007]
37. MacMillan AJ et al. Practical and selective sp^3 C—H bond chlorination via aminium radicals. Angew. Chem. Int. Ed 60, 7132–7139 (2021).
38. Xiang M et al. Visible light-catalyzed benzylic C—H bond chlorination by a combination of organic dye (Acr^+-Mes) and *N*-chlorosuccinimide. J. Org. Chem 85, 9080–9087 (2020). [PubMed: 32434320]
39. Ozawa J & Kanai M Silver-catalyzed C(sp^3)—H chlorination. Org. Lett 19, 1430–1433 (2017). [PubMed: 28256138]
40. Quiclet-Sire B & Zard SZ The xanthate route to amines, anilines, and other nitrogen compounds. A brief account. Synlett. 27, 680–701 (2016).
41. Huang X & Groves JT Oxygen activation and radical transformations in heme proteins and metallophorphyrins. Chem. Rev 118, 2491–2553 (2018). [PubMed: 29286645]
42. Leising RA, Norman RE & Que L Jr. Alkane functionalization by non-porphyrin iron complexes: Mechanistic insights. Inorg. Chem 29, 2553–2555 (1990).
43. Chen K, Costas M & Que L Jr. Spin state tuning of non-heme iron-catalyzed hydrocarbon oxidations: Participation of FeIII–OOH and FeV=O intermediates. J. Chem. Soc., Dalton Trans 672–679 (2002).

44. Kim J, Kim C, Harrison RG, Wilkinson EC & Que L Jr. Fe(TPA)-catalyzed alkane hydroxylation can be a metal-based oxidation. J. Mol. Catal. A: Chem 117, 83–89 (1997).
45. Chen K & Que L Jr. Stereospecific alkane hydroxylation by non-heme iron catalysts: Mechanistic evidence for an FeV=O active species. J. Am. Chem. Soc 123, 6327–6337 (2001). [PubMed: 11427057]
46. Costas M, Tipton AK, Chen K, Jo D-H & Que L Jr. Modeling Rieske dioxygenases: The first example of iron-catalyzed asymmetric cis-dihydroxylation of olefins. J. Am. Chem. Soc 123, 6722–6723 (2001). [PubMed: 11439071]
47. Kim C, Chen K, Kim J & Que L Jr. Stereospecific alkane hydroxylation with H_2O_2 catalyzed by an iron(II)–tris(2-pyridylmethyl)amine complex. J. Am. Chem. Soc 119, 5964–5965 (1997).
48. Costas M & Que L Jr. Ligand topology tuning of iron-catalyzed hydrocarbon oxidations. Angew. Chem. Int. Ed 41, 2179–2181 (2002).
49. Chen MS & White MC A predictably selective aliphatic C—H oxidation reaction for complex molecule synthesis. Science. 318, 783–787 (2007). [PubMed: 17975062]
50. St John P, Guan Y, Kim Y, Kim S, Paton RS Prediction of homolytic bond dissociation enthalpies for organic molecules at near chemical accuracy with sub-second computational cost. Nat. Commun 11, 2328, (2020). [PubMed: 32393773]
51. Chen MS & White MC Combined effects on selectivity in Fe-catalyzed methylene oxidation. Science. 327, 566–571 (2010). [PubMed: 20110502]
52. Gormisky PE & White MC Catalyst-controlled aliphatic C—H oxidations with a predictive model for site-selectivity. J. Am. Chem. Soc 135, 14052–14055 (2013). [PubMed: 24020940]
53. Howell JM, Feng K, Clark JR, Trzepkowski LJ & White MC Remote oxidation of aliphatic C—H bonds in nitrogen-containing molecules. J. Am. Chem. Soc 137, 14590–14593 (2015). [PubMed: 26536374]
54. Osberger TJ, Rogness DC, Kohrt JT, Stepan AF & White MC Oxidative diversification of amino acids and peptides by small-molecule iron catalysis. Nature 537, 214–219 (2016). [PubMed: 27479323]
55. Dantignana V et al. Chemoselective aliphatic C—H bond oxidation enabled by polarity reversal. ACS Cent. Sci 3, 1350–1358 (2017). [PubMed: 29296677]
56. Borrell M, Gil-Caballero S, Bietti M & Costas M Site-selective and product chemoselective aliphatic C—H bond hydroxylation of polyhydroxylated substrates. ACS. Catal 10, 4702–4709 (2020).
57. Zhao J, Nanjo T, de Luca EC & White MC Chemoselective methylene oxidation in aromatic molecules. Nature Chem. 11, 213–221 (2019). [PubMed: 30559371]
58. Milan M, Bietti M & Costas M Highly enantioselective oxidation of nonactivated aliphatic C—H bonds with hydrogen peroxide catalyzed by manganese complexes. ACS. Cent. Sci 3, 196–204 (2017). [PubMed: 28386597]
59. White MC, Doyle AG & Jacobsen EN A synthetically useful, self-assembling MMO mimic system for catalytic alkene epoxidation with aqueous H_2O_2. J. Am. Chem. Soc 123, 7194–7195 (2001). [PubMed: 11459514]
60. Oloo WN & Que L Jr. Bioinspired nonheme iron catalysts for C—H and C=C bond oxidation: Insights into the nature of the metal-based oxidants. Acc. Chem. Res 48, 2612–2621 (2015). [PubMed: 26280131]
61. Kal S, Xu S & Que L Jr. Bio-inspired nonheme iron oxidation catalysis: Involvement of oxoiron(V)oxidants in cleaving strong C—H bonds. Angew. Chem. Int. Ed 59, 7332–7349 (2020).
62. Liu W & Groves JT Manganese catalyzed C—H halogenation. Acc. Chem Res 48, 1727–1735 (2015). [PubMed: 26042637]
63. Liu W et al. Oxidative aliphatic C—H fluorination with fluoride ion catalyzed by a manganese porphyrin. Science. 337, 1322–1325 (2012). [PubMed: 22984066]
64. Li G, Dilger AK, Cheng PT, Ewing WR and Groves JT Selective C—H halogenation with a highly fluorinated manganese porphyrin. Angew. Chem. Int. Ed 57, 1251–1255 (2018).
65. Liu W et al. Site-selective 18F fluorination of unactivated C—H bonds mediated by a manganese porphyrin. Chem. Sci 9, 1168–1172 (2018). [PubMed: 29675161]

66. Huang X, Bergsten TM & Groves JT Manganese-catalyzed late-stage aliphatic C—H azidation. J. Am. Chem. Soc 137, 5300–5303 (2015). [PubMed: 25871027]
67. Huang X et al. Alkyl isocyanates via manganese-catalyzed C—H activation for the preparation of substituted ureas. J. Am. Chem. Soc 139, 15407–15413 (2017). [PubMed: 28976738]
68. Ishii Y, Sakaguchi S & Iwahama T Innovation of hydrocarbon oxidation with molecular oxygen and related reactions. Adv. Synth. Catal 343, 393–427 (2001).
69. Sterckx H, Morel B & Maes BUW Catalytic aerobic oxidation of $C(sp^3)$—H bonds. Angew. Chem. Int. Ed 58, 7946–7970 (2019).
70. Ishii Y; Iwahama T; Sakaguchi S; Nakayama K & Nishiyama Y Alkane oxidation with molecular oxygen using a new efficient catalytic system: *N*-hydroxyphthalimide (NHPI) combined with $Co(acac)_n$ (n = 2 or 3). J. Org. Chem 61, 4520–4526 (1996). [PubMed: 11667375]
71. Hruszkewycz DP, Miles KC, Thiel OR & Stahl SS Co/NHPI-mediated oxygenation of benzylic C—H bonds in pharmaceutically relevant molecules. Chem. Sci 8, 1282–1287 (2017). [PubMed: 28451270]
72. Cooper JC, Luo C, Kameyama R & Van Humbeck JF Combined iron/hydroxytriazole dual catalytic system for site selective oxidation adjacent to azaheterocycles. J. Am. Chem. Soc 140, 1243–1246 (2018). [PubMed: 29345461]
73. Gaster E, Kozuch S & Pappo D Selective aerobic oxidation of methylarenes to benzaldehydes catalyzed by *N*-hydroxyphthalimide and cobalt(II) acetate in hexafluoropropan-2-ol. Angew. Chem. Int. Ed 56, 5912–5915 (2017).
74. Schultz DM et al. Oxyfunctionalization of the remote C—H bonds of aliphatic amines by decatungstate photocatalysis. Angew. Chem. Int. Ed 56, 15274–15278 (2017).
75. Wu W et al. ($n$$Bu_4N$)$W_{10}O_{32}$-catalyzed selective oxygenation of cyclohexane by molecular oxygen under visible light irradiation. Appl. Catal. B: Environ 164, 113–119 (2015).
76. Laudadio G et al. Selective $C(sp^3)$—H aerobic oxidation enabled by decatungstate photocatalysis in flow. Angew. Chem. Int. Ed 57, 4078–4082 (2018).
77. Lee JM, Park J, Cho SH & Chang S Cu-facilitated C—O bond formation using *N*-hydroxyphthalimide: Efficient and selective functionalization of benzyl and allylic C—H bonds. J. Am. Chem. Soc 130, 7824–7825 (2008). [PubMed: 18512912]
78. Guo Z, Jin C, Zhou J & Su W Copper(II)-catalyzed cross dehydrogenative coupling reaction of N-hydroxyphthalimide with alkanes and ethers via unactivated $C(sp^3)$—H activation at room temperature. RSC. Adv 6, 79016–79019 (2016).
79. Zhang X, Yang H & Tang P Transition-metal-free oxidative aliphatic C—H azidation. Org. Lett 17, 5828–5831 (2015). [PubMed: 26569439]
80. Kim K, Lee S & Hong SH Direct $C(sp^3)$—H cyanation enabled by highly active decatungstate photocatalyst. Org. Lett 23, 5501–5505 (2021). [PubMed: 34228456]
81. Sarver PJ, Bissonnette NB & MacMillan DWC Decatungstate-catalyzed $C(sp^3)$—H sulfinylation: Rapid access to diverse organosulfur functionality. J. Am. Chem. Soc 143, 9737–9743 (2021). [PubMed: 34161084]
82. Schirmer TE, Rolka AB, Karl TA, Holzhausen F & König B Photocatalytic C—H trifluoromethylthiolation by the decatungstate anion. Org. Lett 23, 5729–5733 (2021). [PubMed: 34260256]
83. Capaldo L & Ravelli D Decatungstate as direct hydrogen atom transfer photocatalyst for SOMOphilic alkynylation. Org. Lett 23, 2243–2247 (2021). [PubMed: 33656899]
84. Mao R; Bera S; Turla AC & Hu X Copper-catalyzed intermolecular functionalization of unactivated $C(sp^3)$—H bonds and aliphatic carboxylic acids. J. Am. Chem. Soc 143, 14667–14675 (2021). [PubMed: 34463489]
85. Bentley KW, Dummit KA & Van Humbeck JF A highly site-selective radical sp^3 C—H amination of azaheterocycles. Chem. Sci 9, 6440–6445 (2018). [PubMed: 30310574]
86. Hu A, Guo J-J, Pan H & Zuo Z Selective functionalization of methane, ethane, and higher alkanes by cerium photocatalysis. Science 361, 668–672 (2018). [PubMed: 30049785]
87. An Q et al. Cerium-catalyzed C—H functionalizations of alkanes utilizing alcohols as hydrogen atom transfer agents. J. Am. Chem. Soc 142, 6216–6226 (2020). [PubMed: 32181657]

88. Yang Q et al. Photocatalytic C—H activation and the subtle role of chlorine radical complexation in reactivity. Science 372, 847–852 (2021). [PubMed: 34016778]

89. Ryu I et al. Efficient C—H/C—N and C—H/C—CO—N conversion via decatungstate-photoinduced alkylation of diisopropyl azodicarboxylate. Org. Lett 15, 2554–2557 (2013). [PubMed: 23651042]

90. Bonassi F, Ravelli D, Protti S & Fagnoni M Decatungstate photocatalyzed acylations and alkylations in flow via hydrogen atom transfer. Adv. Synth. Catal 357, 3687–3695 (2015).

91. Wan T et al. . Accelerated and scalable C(sp^3)—H amination via decatungstate photocatalysis using a flow photoreactor equipped with high-intensity LEDs. ACS Cent. Sci Accepted Article (2021) 10.1021/acscentsci.1c01109.

92. Giese B Formation of CC bonds by addition of free radicals to alkenes. Angew. Chem. Int. Ed. Engl 22, 753–764 (1983).

93. Crespi S & Fagnoni M Generation of alkyl radicals: From the tyranny of tin to the photon democracy. Chem. Rev 120, 9790–9833 (2020). [PubMed: 32786419]

94. Kanegusuku ALG & Roizen JL Recent advances in photoredox-mediated radical conjugate addition reactions: An expanding toolkit for the Giese reaction. Angew. Chem. Int. Ed 60, 2–36 (2021).

95. Treacy SM & Rovis T Copper-catalyzed C(sp^3)—H bond alkylation via photoinduced ligand-to-metal charge transfer. J. Am. Chem. Soc 143, 2729–2735 (2021). [PubMed: 33576606]

96. Kang YC, Treacy SM & Rovis T Iron-catalyzed photoinduced LMCT: A 1° C—H abstraction enables skeletal rearrangements and C(sp^3)—H alkylation. ACS. Catal 11, 7442–7449 (2021). [PubMed: 35669035]

97. Angioni S et al. Tetrabutylammonium decatungstate (chemo)selective photocatalyzed, radical C—H functionalization in amides. Adv. Synth. Catal 350, 2209–2214 (2008).

98. Yamada K et al. Photocatalyzed site-selective C—H to C—C conversion of aliphatic nitriles. Org. Lett 17, 1292–1295 (2015). [PubMed: 25692554]

99. Fukuyama T et al. Photocatalyzed site-selective C(sp^3)—H functionalization of alkylpyridines at non-benzylic positions. Org. Lett 19, 6436–6439 (2017). [PubMed: 29154551]

100. Fukuyama T, Nishikawa T & Ryu I Site-selective C(sp^3)—H functionalization of fluorinated alkanes driven by polar effects using a tungstate photocatalyst. Eur. J. Org. Chem 1424–1428 (2020).

101. Laudadio G et al. C(sp^3)—H functionalizations of light hydrocarbon using decatungstate photocatalysis in flow. Science 369, 92–96 (2020). [PubMed: 32631892]

102. Roberts BP Polarity-reversal catalysis of hydrogen-atom abstraction reactions: Concepts and applications in organic chemistry. Chem. Soc. Rev 28, 25–35 (1999).

103. Lei G, Xu M, Chang R, Funes-Ardoiz I & Ye J Hydroalkylation of unactivated olefins via visible-light-driven dual hydrogen atom transfer catalysis. J. Am. Chem. Soc 143, 11251–11261 (2021). [PubMed: 34269582]

104. Minisci F, Bernardi R, Bertini F, Galli R, Perchinummo M Nucleophilic character of alkyl radicals—VI: A new convenient selective alkylation of heteroaromatic bases. Tetrahedron 27, 3575–3579 (1971).

105. Proctor RSJ & Phipps RJ Recent advances in Minisci-type reactions. Angew. Chem. Int. Ed 58, 13666–13699 (2019).

106. Leonov D & Elad D Ultraviolet- and γ-ray-induced reactions of nucleic acid constituents. Reactions of purines with ethers and dioxolane. J. Org. Chem 39, 1470–1473 (1974). [PubMed: 4833505]

107. Deng G, Ueda K, Yanagisawa S, Itami K & Li C-J Coupling of nitrogen heteroaromatics and alkanes without transition metals: A new oxidative cross-coupling at C—H/C—H bonds. Chem. Eur. J 15, 333–337 (2009). [PubMed: 19035592]

108. Xia R, Niu H-Y, Qu G-R & Guo H-M CuI controlled C—C and C—N bond formation of heteroaromatics through C(sp^3)—H activation. Org. Lett 14, 5546–5549 (2012). [PubMed: 23072561]

109. Shao X, Wu X, Wu S & Zhu C Metal-free radical-mediated C(sp^3)—H heteroarylation of alkanes. Org. Lett 22, 7450–7454 (2020). [PubMed: 32969219]

110. Tzirakis MD, Lykakis IN & Orfanopoulos M Decatungstate as an efficient photocatalyst in organic chemistry. Chem. Soc. Rev 38, 2609–2621 (2009). [PubMed: 19690741]
111. Quattrini MC et al. Versatile cross-dehydrogenative coupling of heteroaromatics and hydrogen donors *via* decatungstate photocatalysis. Chem. Commun 53, 2335–2338 (2017).
112. De Waele V, Poizat O, Fagnoni M, Bagno A & Ravelli D Unraveling the key features of the reactive state of decatungstate anion in hydrogen atom transfer (HAT) photocatalysis. ACS Catal. 6, 7174–7182 (2016).
113. Ravelli D, Fagnoni M, Fukuyama T, Nishikawa T & Ryu I Site-selective C—H functionalization by decatungstate anion photocatalysis: Synergistic control by polar and steric effects expands the reaction scope. ACS Catal. 8, 701–703 (2018).
114. Li G-X, Hu X, He G & Chen G Photoredox-mediated Minisci-type alkylation of *N*-heteroarenes with alkanes with high methylene selectivity. ACS Catal. 8, 11847–11853 (2018).
115. Lee W, Jung S, Kim M & Hong S Site-selective direct C—H pyridylation of unactivated alkanes by triplet excited anthraquinone. J. Am. Chem. Soc 143, 3003–3012 (2021). [PubMed: 33557526]
116. Shu C, Noble A & Aggarwal VK Metal-free photoinduced C(sp^3)—H borylation of alkanes. Nature 586, 714–719 (2020). [PubMed: 33116286]
117. Kharasch MS & Sosnovsky G The reactions of *t*-butyl perbenzoate and olefins – a stereospecific reaction. J. Am. Chem. Soc 80, 756 (1958).
118. Kharasch M & Fono A Radical substitution reactions. J. Org. Chem 23, 325–326 (1958).
119. Kochi JK Copper salt-catalyzed reaction of butenes with peresters. J. Am. Chem. Soc 84, 774–784 (1962).
120. Muzart J Enantioselective copper-catalyzed allylic acetoxylation of cyclohexene. J. Mol. Catal 64, 381–384 (1991).
121. Andrus MB, Argade AB, Chen X & Pamment MG The asymmetric Kharasch reaction. Catalytic enantioselective allylic acyloxylation of olefins with chiral copper(I) complexes and *tert*-butyl perbenzoate. Tetrahedron Lett. 36, 2945–2948 (1995).
122. Gokhale AS, Minidis ABE & Pfaltz A Enantioselective allylic oxidation catalyzed by chiral bisoxazoline-copper complexes. Tetrahedron Lett. 36, 1831–1834 (1995).
123. Kawasaki K, Tsumura S & Katsuki T Enantioselective allylic oxidation using biomimetic tris(oxazolines)-copper(II) complex. Synlett. 1245–1246 (1995).
124. Andrus MB & Zhou Z Highly enantioselective copper–bisoxazoline-catalyzed allylic oxidation of cyclic olefins with *tert*-butyl *p*-nitroperbenzoate. J. Am. Chem. Soc 124, 8806–8807 (2002). [PubMed: 12137528]
125. Corey EJ & Lee J Enantioselective total synthesis of oleanolic acid, erythrodiol, *β*-amyrin, and other pentacyclic triterpenes from a common intermediate. J. Am. Chem. Soc 115, 8873–8874 (1993).
126. Neukirch H et al. Improved anti-inflammatory activity of three new terpenoids derived, by systematic chemical modifications, from the abundant triterpenes of the flowery plant calendula officinalis. Chem. Biodiversity 2, 657–671 (2005).
127. García-Cabeza AL et al. Allylic oxidation of alkenes catalyzed by a copper–aluminum mixed oxide. Org. Lett 16, 1598–1601 (2014). [PubMed: 24597600]
128. García-Cabeza AL et al. Optimization by response surface methodology (RSM) of the Kharasch–Sosnovsky oxidation of valencene. Org. Process Res. Dev 19, 1662–1666 (2015).
129. Gephart RT et al. Reaction of CuI with dialkyl peroxides: Cu^{II}-alkoxides, alkoxy radicals, and catalytic C—H etherification. J. Am. Chem. Soc 134, 17350–17353 (2012). [PubMed: 23009158]
130. Tran BL, Driess M & Hartwig JF Copper-catalyzed oxidative dehydrogenative carboxylation of unactivated alkanes to allylic esters via alkenes. J. Am. Chem. Soc 136, 17292–17301 (2014). [PubMed: 25389772]
131. Kohmura Y, Kawasaki K & Katsuki T Benzylic and allylic amination. Synlett. 12, 1456–1458 (1997).

132. Pelletier G & Powell DA Copper-catalyzed amidation of allylic and benzylic C—H bonds. Org. Lett 8, 6031–6034 (2006). [PubMed: 17165922]
133. Powell DA & Fan H Copper-catalyzed amination of primary benzylic C—H bonds with primary and secondary sulfonamides. J. Org. Chem 75, 2726–2729 (2010). [PubMed: 20297848]
134. Wiese S et al. Catalytic C—H amination with unactivated amines through copper(II) amides. Angew. Chem. Int. Ed 49, 8850–8855 (2010).
135. Tran BL, Li B, Driess M & Hartwig JF Copper-catalyzed intermolecular amidation and imidation of unactivated alkanes. J. Am. Chem. Soc 136, 2555–2563 (2014). [PubMed: 24405209]
136. Zheng Y-W, Narobe R, Donabauer K, Yabukov S, & König B Copper(II)-photocatalyzed N—H alkylation with alkanes. ACS. Catal 10, 8582–8589 (2020).
137. Borduas N & Powell DA Copper-catalyzed oxidative coupling of benzylic C—H bonds with 1,3-dicarbonyl compounds. J. Org. Chem 73, 7822–7825 (2008). [PubMed: 18767808]
138. Song Z-Q et al. Photoredox oxo-C(sp^3)—H bond functionalization via in situ Cu(I)-acetylide catalysis. Org. Lett 22, 832–836 (2020). [PubMed: 31916774]
139. Vasilopoulos A, Zultanski SL & Stahl SS Feedstocks to pharmacophores: Cu-catalyzed oxidative arylation of inexpensive alkylarenes enabling direct access to diarylalkanes. J. Am. Chem. Soc 139, 7705–7708 (2017). [PubMed: 28555493]
140. Xie W, Heo J, Kim D & Chang S Copper-catalyzed direct C—H alkylation of polyfluoroarenes by using hydrocarbons as an alkylating source. J. Am. Chem. Soc 142, 7487–7496 (2020). [PubMed: 32233362]
141. Ni Z et al. Highly regioselective copper-catalyzed benzylic C—H amination by *N*-fluorobenzenesulfonimide. Angew. Chem. Int. Ed 51, 1244–1247 (2012).
142. Zhang W et al. Enantioselective cyanation of benzylic C—H bonds via copper-catalyzed radical relay. Science, 353, 1014–1018 (2016). [PubMed: 27701109]
143. Xiao H et al. Copper-catalyzed late-stage benzylic C(sp^3)—H trifluoromethylation. Chem. 5, 940–949 (2019).
144. Suh S-E et al. Site-selective copper-catalyzed azidation of benzylic C—H bonds. J. Am. Chem. Soc 142, 11388–11393 (2020). [PubMed: 32539355]
145. Sharma A & Hartwig JF Metal-catalyzed azidation of tertiary C—H bonds suitable for late-stage functionalization. Nature 517, 600–604 (2015). [PubMed: 25631448]
146. Margrey KA, Czaplyski WL, Nicewicz DA & Alexanian EJ A general strategy for aliphatic C—H functionalization enabled by organic photoredox catalysis. J. Am. Chem. Soc 140, 4213–4217 (2018). [PubMed: 29522330]
147. Liu S et al. Copper-catalyzed oxidative benzylic C(sp^3)—H amination: Direct synthesis of benzylic carbamates. Chem. Commun 56, 13013–13016 (2020).
148. Wang A, DeOliveira CC & Emmert M Non-directed, copper catalyzed benzylic C—H amination avoiding substrate excess. ChemRxiv. Preprint at 10.26434/chemrxiv.8792243.v2 (2019).
149. Jiang C, Chen P & Liu G Copper-catalyzed benzylic C—H bond thiocyanation: Enabling late-stage diversifications. CCS Chem. 2, 1884–1893 (2020).
150. Suh S-E, Nkulu LE, Lin S, Krska SW & Stahl SS Benzylic C—H isocyanation/amine coupling sequence enabling high-throughput synthesis of pharmaceutically relevant ureas. Chem. Sci 12, 10380–10387 (2021). [PubMed: 34377424]
151. Vasilopoulos A, Golden DL, Buss JA & Stahl SS Copper-catalyzed C—H fluorination/functionalization sequence enabling benzylic C—H cross coupling with diverse nucleophiles. Org. Lett 22, 5753–5757 (2020). [PubMed: 32790420]
152. Champagne PA et al. Enabling nucleophilic substitution reactions of activated alkyl fluorides through hydrogen bonding. Org. Lett 15, 2210–2213 (2013). [PubMed: 23614350]
153. Champagne PA, Benhassine Y, Desroches J & Paquin J-P Friedel–Crafts reaction of benzyl fluorides: Selective activation of C—F bonds as enabled by hydrogen bonding. Angew. Chem. Int. Ed 53, 13835–13839 (2014).
154. Hemelaere R, Champagne PA, Desroches J & Paquin J-F Faster initiation in the Friedel–Crafts reaction of benzyl fluorides using trifluoroacetic acid as activator. J. Fluorine Chem 190, 1–6 (2016).

155. Hamel J-D & Paquin J-F Activation of C—F bonds α to C—C multiple bonds. Chem. Commun 54, 10224–10239 (2018).
156. Lopez MA, Buss JA & Stahl SS Site-selective chlorination of benzylic C—H bonds by Cu-catalysis. Org. Lett 24, (2022), in press, DOI: 10.1021/acs.orglett.1c04038.
157. Jin J et al. Copper(I)-catalysed site-selective C(sp^3)—H bond chlorination of ketones, (*E*)-enones and alkylbenzenes by dichloramine-T. Nat. Commun 12, 4065 (2021). [PubMed: 34210971]
158. Fawcett A, Keller MJ, Herrera Z & Hartwig JF Site selective chlorination of C(sp^3)—H bonds suitable for late-stage functionalization. Angew. Chem. Int. Ed 60, 8276–8283 (2021).
159. Li J et al. Site-specific allylic C—H bond functionalization with a copper-bound N-centered radical. Nature 574, 516–521 (2019). [PubMed: 31645723]
160. Zhou J, Jin C, Li X & Su W Copper-catalyzed oxidative esterification of unactivated C(sp^3)—H bonds with carboxylic acids via cross dehydrogenative coupling. RCS Adv. 5, 7232–7236 (2015).
161. Hu H et al. Copper-catalyzed benzylic C—H coupling with alcohols via radical relay enabled by redox buffering. Nat. Catal 3, 358–367 (2020). [PubMed: 32368720]
162. Chen S-J, Golden DL, Krska SW & Stahl SS Copper-catalyzed cross-coupling of benzylic C—H bonds and azoles with controlled *N*-site selectivity. J. Am. Chem. Soc 143, 14438–14444 (2021). [PubMed: 34464528]
163. Ivanova AE et al. Ambident polyfluoroalkyl-substituted pyrazoles in the methylation reactions. J. Fluorine Chem 195, 47–56 (2017).
164. Huang A et al. Regioselective synthesis, NMR, and crystallographic analysis of N1-substituted pyrazoles. J. Org. Chem 82, 8864–8872 (2017). [PubMed: 28718639]
165. Zhang W, Chen P & Liu G Copper-catalyzed arylation of benzylic C—H bonds with alkylarenes as the limiting reagents. J. Am. Chem. Soc 139, 7709–7712 (2017). [PubMed: 28562032]
166. Zhang W, Wu L, Chen P & Liu G Enantioselective arylation of benzylic C—H bonds by copper-catalyzed radical relay. Angew. Chem. Int. Ed 58, 6425–6429 (2019).
167. Fu L, Zhang Z, Chen P, Lin Z & Liu G Enantioselective copper-catalyzed alkynylation of benzylic C—H bonds via radical relay. J. Am. Chem. Soc142, 12493–12500 (2020). [PubMed: 32539406]
168. Li Z, Cao L & Li C-J $FeCl_2$-catalyzed selective C—C bond formation by oxidative activation of a benzylic C—H bond. Angew. Chem. Int. Ed 46, 6505–6507 (2007).
169. Xia Q, Chen W & Qiu H Direct C—N coupling of imidazoles and benzylic compounds via iron-catalyzed oxidative activation of C—H bonds. J. Org. Chem 76, 7577–7582 (2011). [PubMed: 21797284]
170. Kumar J, Suresh E & Bhadra S Catalytic direct α-amination of arylacetic acid synthons with anilines. J. Org. Chem 85, 13363–13374 (2020). [PubMed: 32998508]
171. Karimov RR, Sharma A & Hartwig JF Late Stage Azidation of Complex Molecules. ACS Cent. Sci 2, 715–724 (2016). [PubMed: 27800554]
172. Ye Y-H, Zhang J, Wang G, Chen S-Y & Yu X-Q Cobalt-catalyzed benzylic C—H amination via dehydrogenative-coupling reaction. Tetrahedron 67, 4649–4654 (2011).
173. Tang S, Wang P, Li H & Lei A Multimetallic catalysed radical oxidative C(sp^3)—H /C(sp)—H cross-coupling between unactivated alkanes and terminal alkynes. Nat. Commun 7, 11676 (2016). [PubMed: 27339161]
174. Liu D, Liu C, Li H & Lei A Direct functionalization of tetrahydrofuran and 1,4-dioxane: Nickel-catalyzed oxidative C(sp^3)—H arylation. Angew. Chem. Int. Ed 52, 4453–4456 (2013).
175. Liu D et al. Nickel-catalyzed oxidative radical cross-coupling: An effective strategy for inert Csp^3—H functionalization. Org. Lett 17, 998–1001 (2015). [PubMed: 25651336]
176. Vasilopoulos A, Krska SW & Stahl SS C(sp^3)—H methylation enabled by peroxide photosensitization and Ni-mediated radical coupling. Science 372, 398–403 (2021). [PubMed: 33888639]
177. Schönherr H & Cernak T Profound methyl effects in drug discovery and a call for new C—H methylation reactions. Angew. Chem. Int. Ed 52, 12256–12267 (2013).
178. Xu P, Guo S, Wang L & Tang P Silver-catalyzed oxidative activation of benzylic C—H bonds for the synthesis of difluoromethylated arenes. Angew. Chem. Int. Ed 126, 6065–6068 (2014).

179. Yang H et al. Silver-promoted oxidative benzylic C—H trifluoromethoxylation. Angew. Chem. Int. Ed 57, 13266013270 (2018).
180. Skubi KL, Blum TR & Yoon TP Dual catalysis strategies in photochemical synthesis. Chem. Soc. Rev 116, 10035–10074 (2016).
181. Twilton J et al. The merger of transition metal and photocatalysis. Nat. Rev. Chem 1, 0052 (2017).
182. Shaw MH, Twilton J & MacMillan DWC Photoredox catalysis in organic chemistry. J. Org. Chem 81, 6898–6926 (2016). [PubMed: 27477076]
183. Levin MD, Kim S & Toste FD Photoredox catalysis unlocks single-electron elementary steps in transition metal catalyzed cross-coupling. ACS Cent. Sci 2, 293–301 (2016). [PubMed: 27280163]
184. Matsui JK, Lang SB, Heitz DR & Molander GA Photoredox-mediated routes to radicals: The value of catalytic radical generation in synthetic methods development. ACS Catal. 7, 2563–2575 (2017). [PubMed: 28413692]
185. McAtee RC, McClain EJ & Stephenson CRJ Illuminating Photoredox Catalysis. Trends Chem. 1, 111–125 (2019).
186. Chan AY et al. Metallaphotoredox: The merger of photoredox and transition metal catalysis. Chem. Rev Accepted Article (2021) 10.1021/acs.chemrev.1c00383.
187. Capaldo L; Ravelli D & Fagnoni M Direct photocatalyzed hydrogen atom transfer (HAT) for aliphatic C—H bonds elaboration. Chem. Rev Accepted Article (2021) 10.1021/acs.chemrev.1c00263.
188. Leibler IN-M, Tekle-Smith MA & Doyle A A general strategy for C(sp^3)—H functionalization with nucleophiles using methyl radical as a hydrogen atom abstractor. Nat. Commun 12, 6950 (2021). [PubMed: 34845207]
189. Zhang Y et al. A photoredox-catalyzed approach for formal hydride abstraction to enable a general Csp^3—H fluorination with HF. Chem. Catalysis 2, 292–308 (2022).
190. Li G-X et al. A unified photoredox-catalysis strategy for C(sp^3)—H hydroxylation and amidation using hypervalent iodine. Chem. Sci 8, 7180–7185 (2017). [PubMed: 29081950]
191. Michaudel Q, Thevenet D & Baran PS Intermolecular Ritter-type C—H amination of unactivated sp^3 carbons. J. Am. Chem. Soc 134, 2547–2550 (2012). [PubMed: 22276612]
192. Kiyokawa K, Takemoto K & Minakata S Ritter-type amination of C—H bonds at tertiary carbon centers using iodic acid as an oxidant. Chem. Commun 52, 13082–13085 (2016).
193. Maeda B, Sakakibara Y, Murakami K & Itami K Photoredox-catalyzed benzylic esterification via radical-polar crossover. Org. Lett 23, 5113–5117 (2021).
194. Meng Q-Y, Schirmer TE, Berger AL, Donabauer K & König B Photocarboxylation of benzylic C—H bonds. J. Am. Chem. Soc 141, 11393–11397 (2019). [PubMed: 31280561]
195. Berger AL, Donabauer K & König B Photocatalytic carbanion generation from C—H bonds – reductant free Barbier/Grignard-type reactions. Chem. Sci 10, 10991–10996 (2019). [PubMed: 34040714]
196. Bosnidou AE & Muñiz K Intermolecular radical C(sp^3)—H amination under iodine catalysis. Angew. Chem. Int. Ed 58, 7485–7489 (2019).
197. Romine AM et al. Easy access to the copper(III) anion $[Cu(CF_3)_4]^-$. Angew. Chem. Int. Ed 54, 2745–2749 (2015).
198. Guo S, AbuSalim DI & Cook SP Aqueous benzylic C—H trifluoromethylation for late-stage functionalization. J. Am. Chem. Soc 140, 12378–12382 (2018). [PubMed: 30247886]
199. He J, Nguyen TN, Guo S & Cook SP Csp^3—H trifluoromethylation of unactivated aliphatic systems. Org. Lett 23, 702–705 (2021). [PubMed: 33443442]
200. Choi G, Lee GS, Park B, Kim D & Hong SH Direct C(sp^3)—H trifluoromethylation of unactivated alkanes enabled by multifunctional trifluoromethyl copper complexes. Angew. Chem. Int. Ed 60, 5467–5474 (2021).
201. Sarver PJ et al. The merger of decatungstate and copper catalysis to enable aliphatic C(sp^3)—H trifluoromethylation. Nat. Chem 12, 459–467 (2020). [PubMed: 32203440]

202. Shaw MH, Shurtleff VW, Terrett JA, Cuthbertson JD & MacMillan DWC Native functionality in triple catalytic cross-coupling: sp^3 C—H bonds as latent nucleophiles. Science 352, 1304–1308 (2016). [PubMed: 27127237]
203. Le C, Liang Y, Evans RW, Li X & MacMillan DWC Selective sp^3 C—H alkylation via polarity-match-based cross-coupling. Nature 547, 79–83 (2017). [PubMed: 28636596]
204. Zhang X & MacMillan DWC Direct aldehyde C—H arylation and alkylation via the combination of nickel, hydrogen atom transfer, and photoredox catalysis. J. Am. Chem. Soc 139, 11353–11356 (2017). [PubMed: 28780856]
205. Twilton J et al. Selective hydrogen atom abstraction through induced bond polarization: Direct α-arylation of alcohols through photoredox, HAT, and nickel catalysis. Angew. Chem. Int. Ed 57, 5369–5373 (2018).
206. Ma Z-Y et al. Sulfonamide as photoinduced hydrogen-atom transfer catalyst for regioselective alkylation of C(sp^3)—H bonds adjacent to heteroatoms. Org. Lett 23, 474–479 (2021). [PubMed: 33373258]
207. Perry IB et al. Direct arylation of strong aliphatic C—H bonds. Nature 560, 70–75 (2018). [PubMed: 30068953]
208. Berger M, Goldblatt IL & Steel C Photochemistry of benzaldehyde. J. Am. Chem. Soc 95, 1717–1725 (1973).
209. Dórman G, Nakamura H Pulsipher A & Prestwich GD The life of pi star: Exploring the exciting and forbidden worlds of the benzophenone photophore. Chem. Rev 116, 15284–15398 (2016). [PubMed: 27983805]
210. Shen Y, Gu Y & Martin R sp^3 C—H arylation and alkylation enabled by the synergy of triplet excited ketones and nickel catalysts. J. Am. Chem. Soc 140, 12200–12209 (2018). [PubMed: 30184423]
211. Dewanji A, Krach PE & Rueping M The dual role of benzophenone in visible-light/nickel photoredox-catalyzed C—H arylations: Hydrogen-atom transfer and energy transfer. Angew. Chem. Int. Ed 58, 3566–3570 (2019).
212. Zhang L et al. The combination of benzaldehyde and nickel-catalyzed photoredox C(sp^3)—H alkylation/arylation. Angew. Chem. Int. Ed 58, 1823–1827 (2019).
213. Si X, Zhang L & Hashmi SK Benzaldehyde- and nickel-catalyzed photoredox C(sp^3)—H alkylation/arylation with amides and thioethers. Org. Lett 21, 6329–6332 (2019). [PubMed: 31373208]
214. Heitz DR, Tellis JC & Molander GA Photochemical nickel-catalyzed C—H arylation: Synthetic scope and mechanistic investigations. J. Am. Chem. Soc 138, 12715–12718 (2016). [PubMed: 27653500]
215. Shields BJ & Doyle AG Direct C(sp^3)—H cross-coupling enabled by catalytic generation of chlorine radicals. J. Am. Chem. Soc 138, 12719–12722 (2016). [PubMed: 27653738]
216. Nielsen MK et al. Mild, redox-neutral formylation of aryl chlorides through the photocatalytic generation of chlorine radicals. Angew. Chem. Int. Ed 56, 7191–7194 (2017).
217. Chang X, Lu H & Lu Z Enantioselective benzylic C—H arylation via photoredox and nickel dual catalysis. Nat. Commun 10, 3549 (2019). [PubMed: 31391466]
218. Cheng X; Li T; Liu Y & Lu Z Stereo- and enantioselective benzylic C—H alkenylation via photoredox/nickel dual catalysis. ACS Catal. 11, 11059–11065 (2021).
219. Joe CL & Doyle AG Direct acylation of C(sp^3)—H bonds enabled by nickel and photoredox catalysis. Angew. Chem. Int. Ed 55, 4040–4043 (2016).
220. Ahneman DT & Doyle AG C—H functionalization of amines with aryl halides by nickel-photoredox catalysis. Chem Sci. 7, 7002–7006 (2016). [PubMed: 28058105]
221. Novaes LF et al. Electrocatalysis as an enabling technology for organic synthesis. Chem. Soc. Rev 50, 7941–8002 (2021). [PubMed: 34060564]
222. Chen N & Xu H-C Electrochemical generation of nitrogen-centered radicals for organic synthesis. Green Synth. Catal 2, 165–178 (2021).
223. Masui M, Hara S, Ueshima T, Kawagushi T & Ozaki S Anodic oxidation of compounds having benzylic or allylic carbon and α-carbon to hetero atom using N-hydroxyphthalimide as a mediator. Chem Pharm. Bull 31, 4209–4211 (1983).

224. Masui M, Hosomi K, Tsuchida K & Ozaki S Electrochemical oxidation of olefins using *N*-hydroxyphthalimide as a mediator. Chem. Pharm. Bull 33, 4798–4802 (1985).

225. Masui M, Hara S & Ozaki S Anodic oxidation of amides and lactams using N-hydroxyphthalimide as a mediator. Chem. Pharm. Bull 34, 975–979 (1986).

226. Nutting JE, Rafiee MR & Stahl SS Tetramethylpiperidine *N*-oxyl (TEMPO), phthalimide *N*-oxyl (PINO), and related *N*-Oxyl species: Electrochemical properties and their use in electrocatalytic reactions. Chem. Rev 118, 4834–4885 (2018). [PubMed: 29707945]

227. Horn EJ et al. Scalable and sustainable electrochemical allylic C—H oxidation. Nature 533, 77–81 (2016). [PubMed: 27096371]

228. Mo Y & Jensen KF Continuous *N*-hydroxyphthalimide (NHPI)-mediated electrochemical aerobic oxidation of benzylic C—H bonds. Chem. Eur. J 24, 10260–10265 (2018).

229. Kawamata Y et al. Scalable, electrochemical oxidation of unactivated C—H bonds. J. Am. Chem. Soc 139, 7448–7451 (2017). [PubMed: 28510449]

230. Saito M et al. N-ammonium ylide mediators for electrochemical C—H oxidation. J. Am. Chem. Soc 143, 7859–7867 (2021). [PubMed: 33983721]

231. Rafiee M, Wang F, Hruszkewycz DP & Stahl SS *N*-hydroxyphthalimide-mediated electrochemical iodination of methylarenes and comparison to electron-transfer-initiated C—H functionalization. J. Am. Chem. Soc 140, 22–25 (2018). [PubMed: 29220181]

232. Hayashi R, Shimizu A & Yoshida J The stabilized cation pool method: Metal- and oxidant-free benzylic C—H/aromatic C—H cross-coupling. J. Am. Chem. Soc 138, 8400–8403 (2016). [PubMed: 27341676]

233. Zhu Y et al. A promising electro-oxidation of methyl-substituted aromatic compounds to aldehydes in aqueous imidazole ionic liquid solutions. J. Electroanal. Chem 751, 105–110 (2015).

234. Das A; Nutting JE & Stahl SS Electrochemical C—H oxygenation and alcohol dehydrogenation involving Fe-oxo species using water as the oxygen source. Chem. Sci 10, 7542–7548 (2019). [PubMed: 31588305]

235. Robinson SG, Mack JBC, Alektiar SN, Du Bois J & Sigman MS Electrochemical ruthenium-catalyzed C—H hydroxylation of amine derivatives in aqueous acid. Org. Lett 22, 7060–7063 (2020). [PubMed: 32419465]

236. Meyer TH, Samanta RC, Del Vecchio A & Ackermann L Mangana(III/IV)electro-catalyzed C(sp^3)—H azidation. Chem. Sci 12, 2890–2897 (2021).

237. Niu L et al. Manganese-catalyzed oxidative azidation of C(sp^3)—H bonds under electrophotocatalytic conditions. J. Am. Chem. Soc 142, 17693–17702 (2020). [PubMed: 32941025]

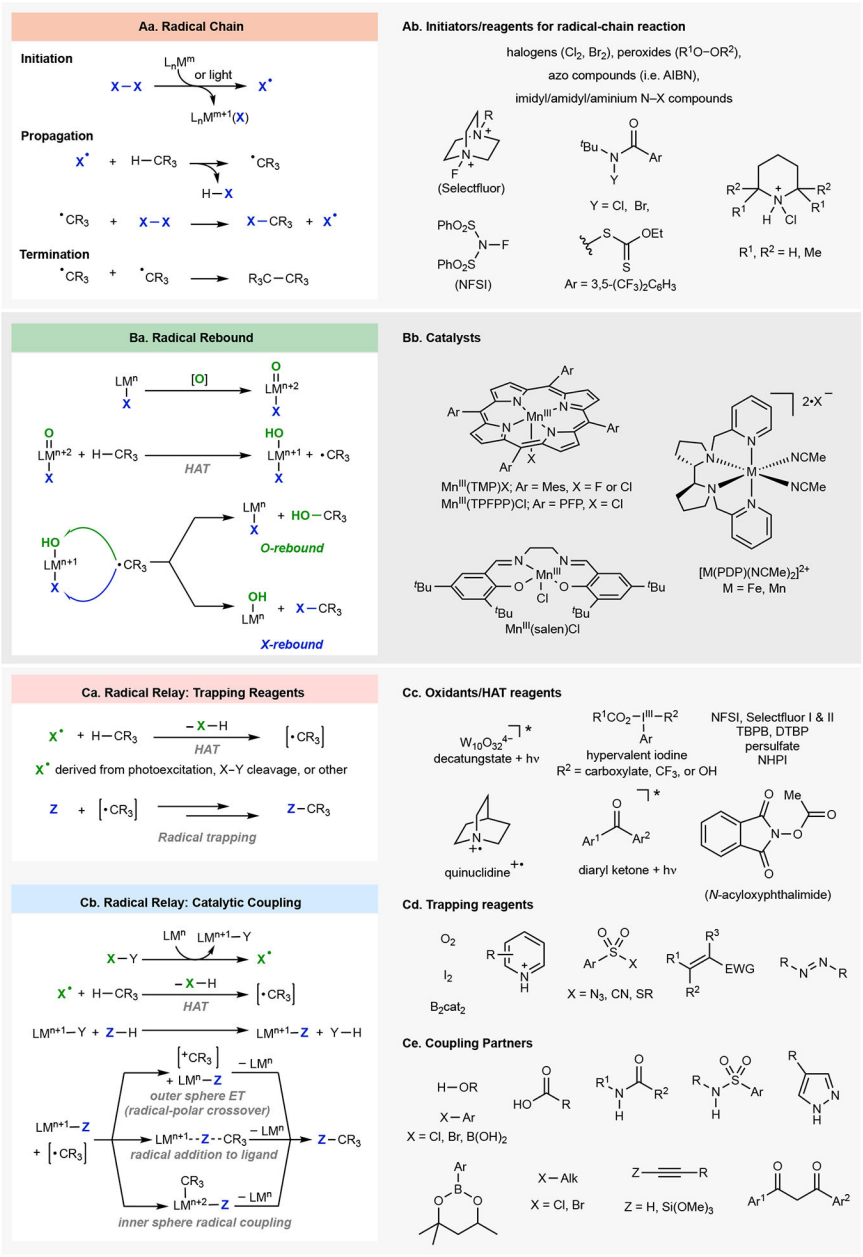

Fig. 1 | Mechanisms and components of radical-chain, radical-rebound, and radical-relay reactions.

Aa | General mechanism of radical-chain reaction. **Ab** | Representative initiators/reagents for radical-chain reactions. **Ba** | General catalytic cycle of radical-rebound reactions. **Bb** | Representative iron and manganese catalysts for radical-rebound reactions. **Ca** | General mechanism of radical-relay reactions involving radical trapping reagents. **Cb** | General mechanism of catalytic radical-relay reactions. **Cc** | Representative oxidants and HAT reagents for radical-relay reactions. **Cd** | Representative radical trapping reagents. **Ce** | Representative catalytic radical-relay coupling partners. [O] = $O_2/2e^-$, H_2O_2, or other O-atom transfer reagent. NFSI, *N*-fluorobenzenesulfonimide; Selectfluor I (R = CH_2Cl), 1-chloromethyl-4-fluoro-1,4-diazoniabicyclo[2.2.2]octane bis(tetrafluoroborate); Selectfluor II

(R = CH_3), 1-fluoro-4-methyl-1,4-diazoniabicyclo[2.2.2]octane bis(tetrafluoroborate); TMP, 5,10,15,20-tetramesitylporphyrin; TPFPP, 5,10,15,20-tetrakis(pentafluorophenyl)porphyrin; PDP, *N,N′*-bis(2-pyridylmethyl)-2,2′-bipyrrolidine; HAT, hydrogen atom transfer; ET, electron transfer; TBPB, *tert*-butyl peroxybenzoate; DTBP, di-*tert*-butyl peroxide; NHPI, *N*-hydroxyphthalimide; B_2cat_2, bis(catecholato)diboron.

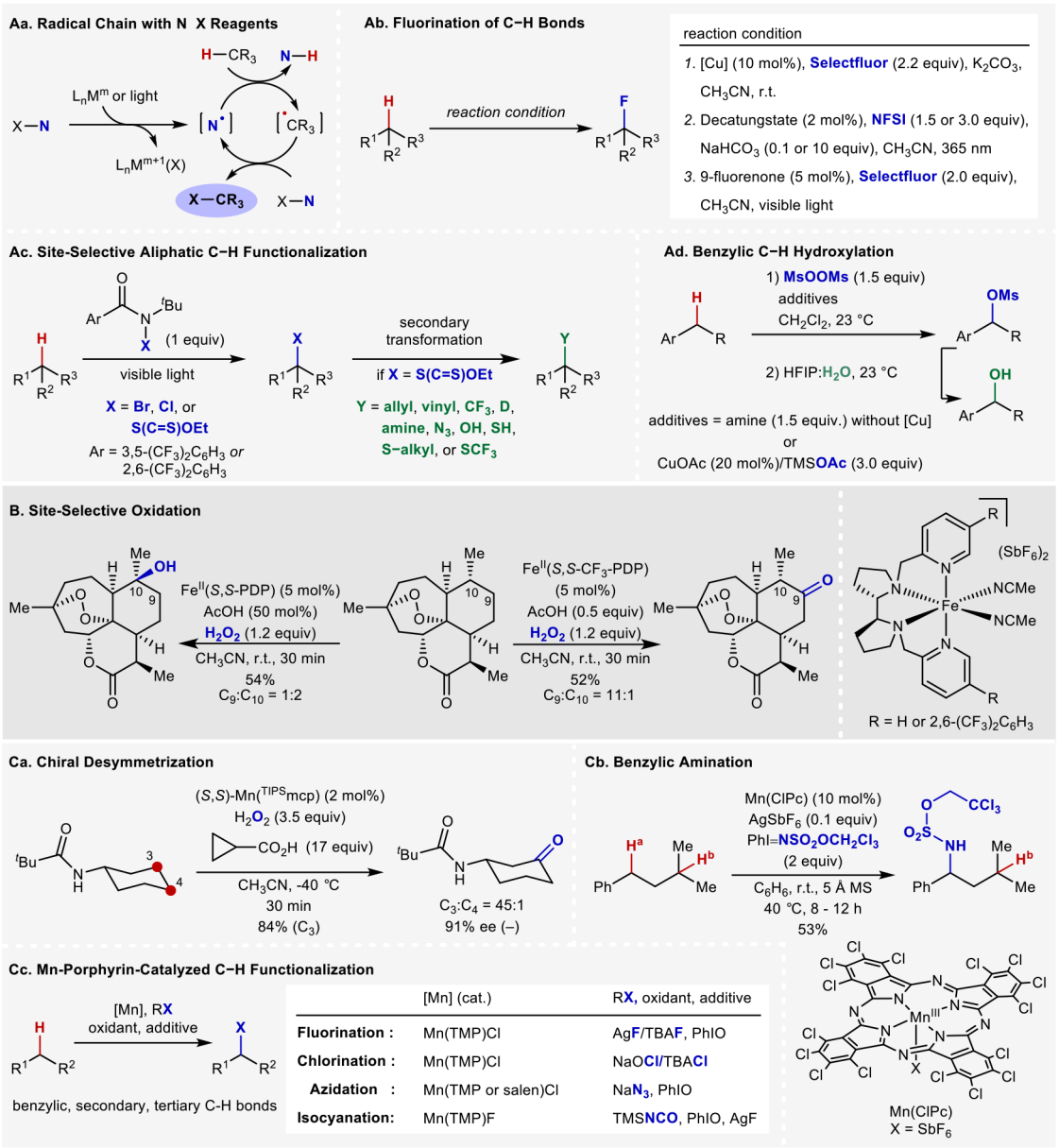

Fig. 2 | Late-stage C(sp^3)—H functionalization reactions via radical chain and radical rebound. **Aa** | General mechanism for radical-chain reaction with a N—X reagent. **Ab** | Fluorination reactions of C(sp^3)—H bonds. **Ac** | Site-selective aliphatic C—H halogenation and xanthylation reactions with N—X reagents. **Ad** | Benzylic C(sp^3)—H hydroxylation reaction. **B** | Iron-catalyzed C—H oxidation reaction. **Ca** | Manganese-non-heme catalyzed chiral desymmetrization of cyclohexane. **Cb** | Manganese-catalyzed benzylic amination reaction. **Cc**| Manganese-porphyrin or -salen catalyzed C—H functionalization reactions. HFIP, hexafluoroisopropanol; PDP, *N*,**N**′-bis(2-pyridylmethyl)-2,2′-bipyrrolidine; ^{TIPS}mcp, *N,N*′-dimethyl *N,N*′-bis(2-(5-triisopropylsilylpyridyl)methyl)-1,2-*trans*-diaminocyclohexane; Pc, phthalocyanine; TMP, 5,10,15,20-tetramesitylporphyrin; TMS, trimethylsilyl.

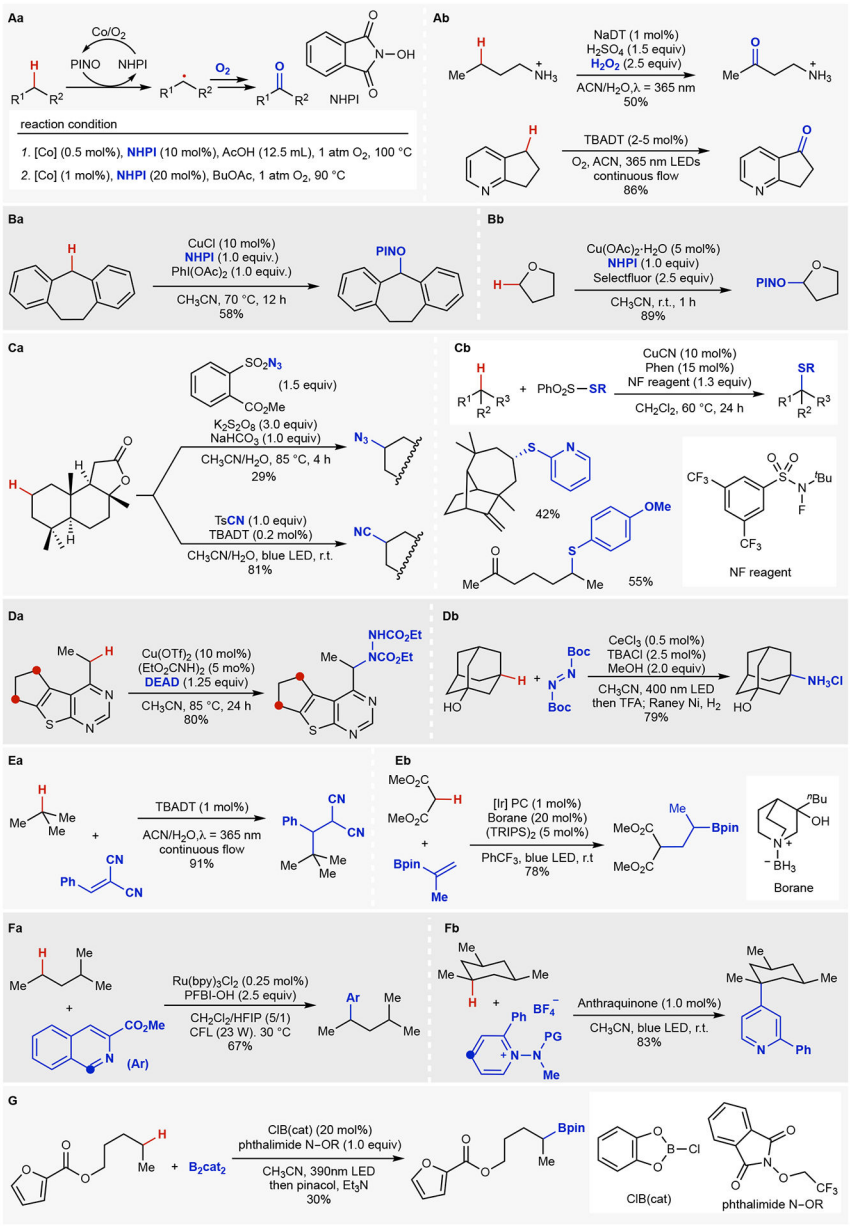

Fig. 3 | Radical relay involving radical addition to trapping reagents.

Aa | Oxygenation with Co/NHPI cocatalysts. **Ab** | Oxygenation with decatungstate photocatalysts. **Ba/b** | PINOylation methods. **Ca** | Azidation/cyanation via radical trapping with sulfonyl–X reagents (X = N_3, CN). **Cb** | Thiol coupling via radical trapping with sulfonylthiolates. **Da** | Amination of heterobenzylic C(sp^3)—H bonds with DEAD. **Db** | Amination initiated by LMCT with Ce^{IV} reagents. **Ea** | Giese-type alkylation with decatungstate photocatalysts. **Eb** | Polarity reversal HAT/Giese-type alkylation. **Fa** | Minisci reaction with decatungstate photocatalyst. **Fb** | Photochemical Minisci-type pyridylation. **G** | Photochemical borylation. NHPI, *N*-hydroxyphthalimide; DEAD, diethyl azodicarboxylate; LMCT, ligand-to-metal charge transfer; TFA, trifluoroacetic acid; $(TRIPS)_2$, bis(2,4,6-triisopropylphenyl) disulfide; PFBI–OH, hydroxyl

perfluorobenziodoxole; HFIP, hexafluoroisopropanol; B_2cat_2, bis(catecholato)diboron; ClB(cat), B-chlorocatecholborane; DT, decatungstate.

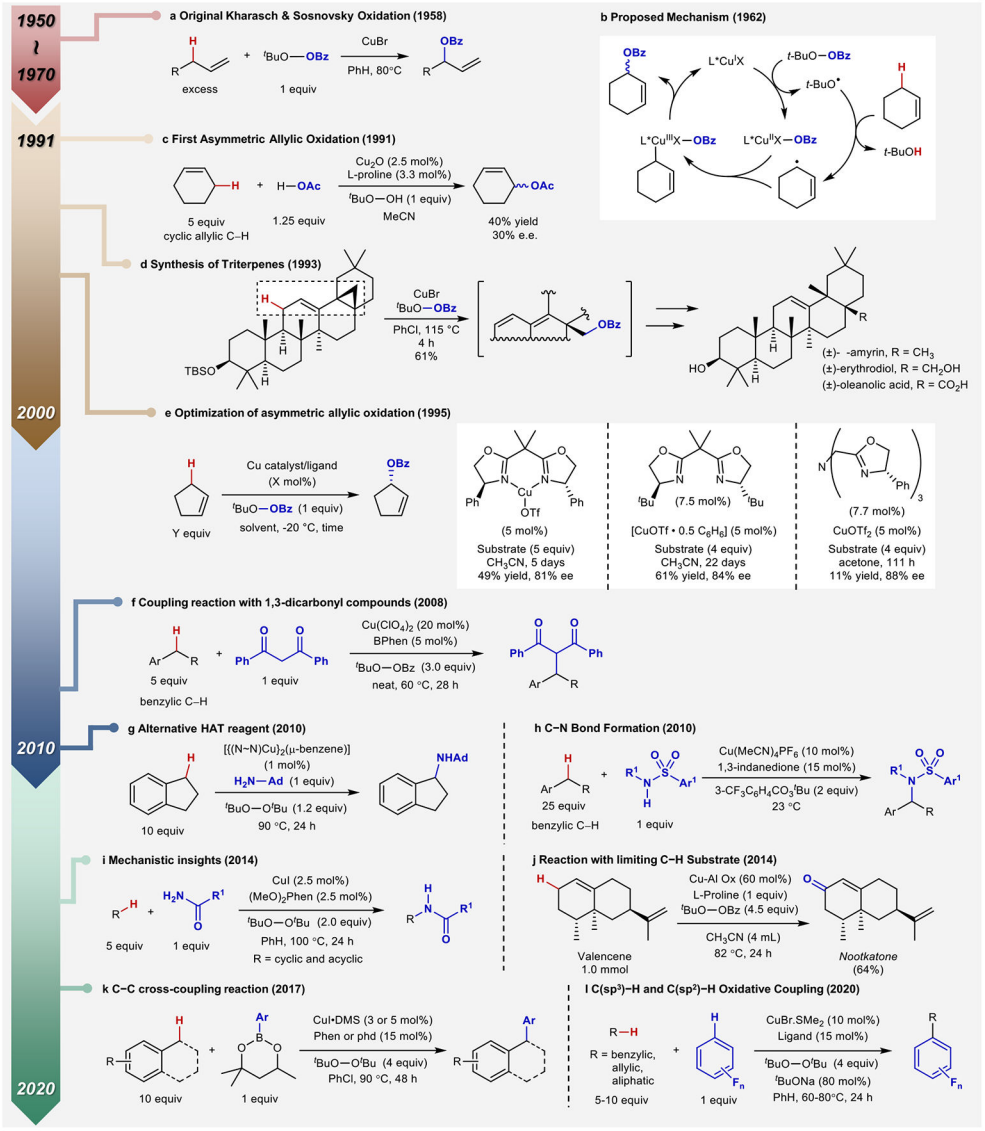

Fig. 4 | Timeline of representative Kharasch-Sosnovsky (K-S)-type reactions.

a | Original Kharasch-Sosnovsky reaction. **b** | Kharasch-Sosnovsky reaction mechanism. **c** | First asymmetric allylic oxidation. **d** | Synthesis of triterpenes. **e** | Examples of asymmetric allylic oxidation. **f** | Cross-coupling reaction of benzylic C—H bonds and 1,3-dicarbonyl compounds. **g** | An alternative HAT reagent. **h** | C—N bond formation reaction. **i** | Mechanistic insights for C—N bond formation. **j** | Allylic oxidation with limiting C—H substrate. **k** | Cross coupling of benzylic C—H bonds and arylboronic esters. **l** | Cross coupling of C(sp^3)—H and C(sp^2)—H bonds. TBS, *tert*-butyldimethylsilyl; BPhen, bathophenanthroline; N~N, β-diketiminate ligand: 2,4-bis-(2,6-dichlorophenylimino)pentyl; Ad, 1-adamantyl; Phen, phenanthroline; phd, 1,10-phenanthroline-5,6-dione.

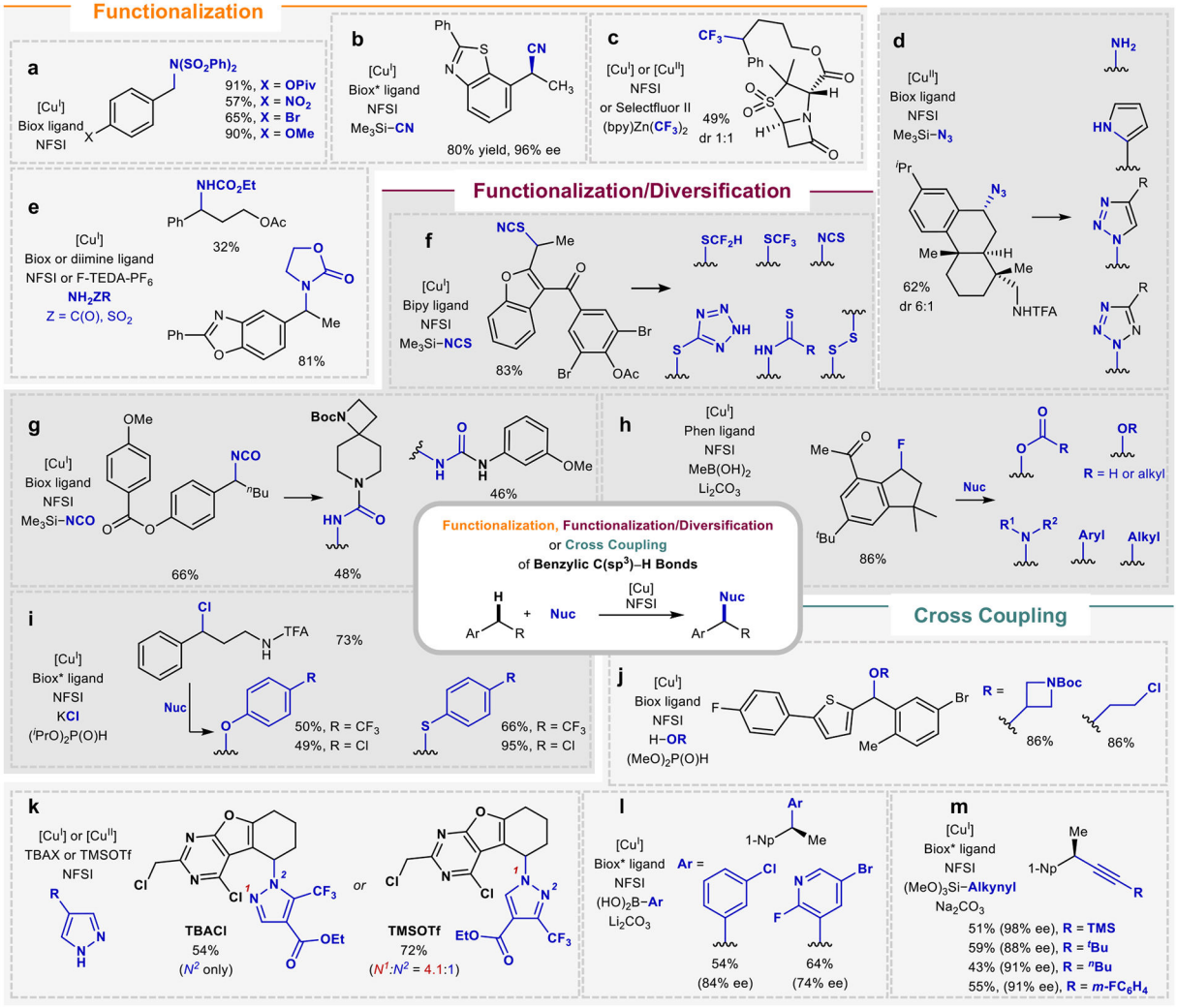

Fig. 5 | Summary of Cu/NFSI-catalyzed radical-relay functionalization, functionalization/diversification, and cross-coupling reactions of benzylic C(sp^3)—H bonds.

a | Sulfonimidation. **b** | Enantioselective cyanation. **c** | Trifluoromethylation. **d** | Azidation reaction. **e** | Amination methods with amides and ammonia surrogates. **f** | Thiocyanation. **g** | Isocyanation/amine coupling sequence. **h** | Fluorination/diversification. **i** | Chlorination/diversification. **j** | Cross coupling of benzylic C—H bonds and alcohols. **k** | Cross coupling of benzylic C—H bonds and azoles with *N*-site selectivity. **l** | Enantioselective cross coupling of benzylic C—H bonds and arylboronic acids. **m** | Enantioselective alkynylation. NFSI, *N*-fluorobenzenesulfonimide; Selectfluor II, 1-fluoro-4-methyl-1,4-diazoniabicylco[2.2.2]octanebis(tetrafluoroborate); 1-Np, 1-naphthalene; TMS, trimethylsilyl; F-TEDA-PF$_6$, 1-chloromethyl-4-fluoro-1,4-diazoniabicyclo[2.2.2]octane bis(hexafluorophosphate); TBACl, tetrabutylammonium chloride; TMSOTf, trimethylsilyl triflate; TFA, trifluoroacetyl-protected amine.

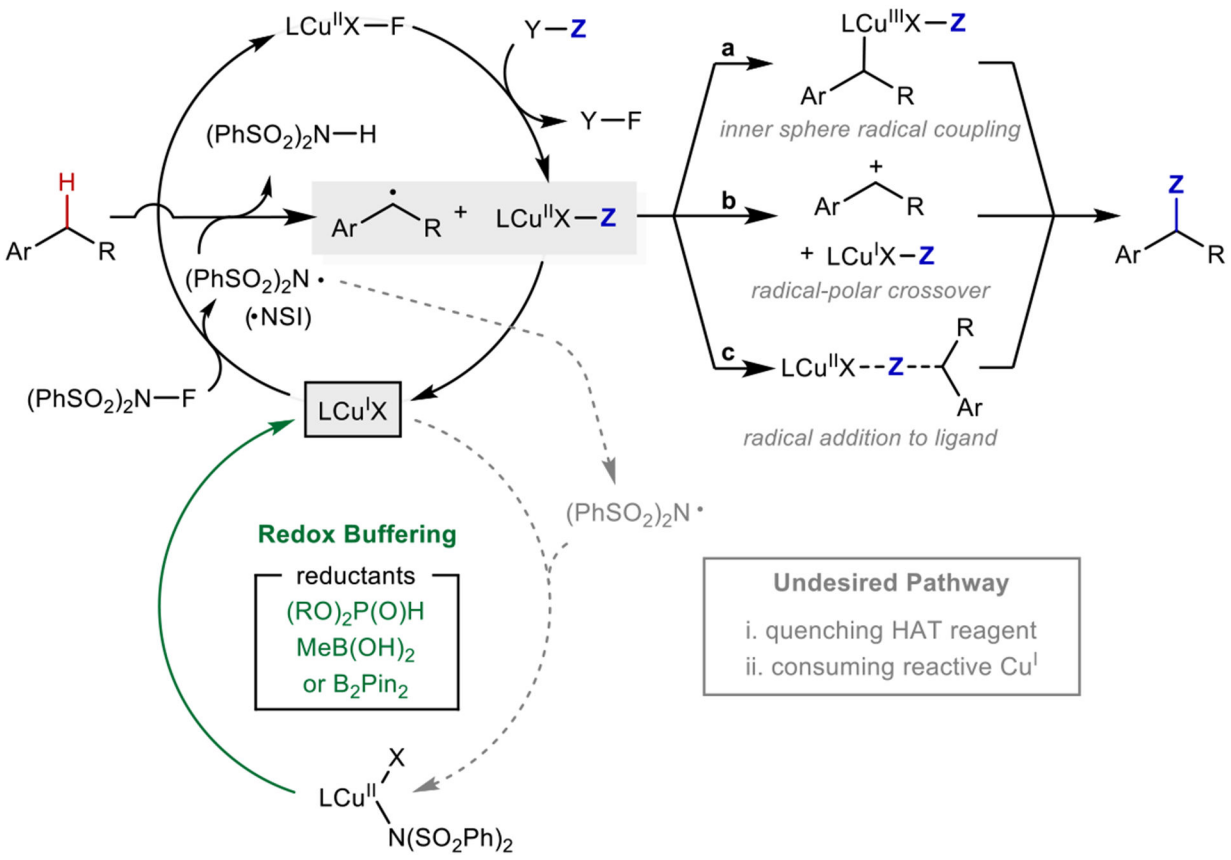

Fig. 6 | . Catalytic cycle and radical functionalization mechanisms for Cu/NFSI-catalyzed radical-relay reactions.

a | Inner sphere radical coupling via reductive elimination. **b** | Radical-polar crossover pathway. **c** | Radical addition to Cu-bound ligand. NFSI, *N*-fluorobenzenesulfonimide.

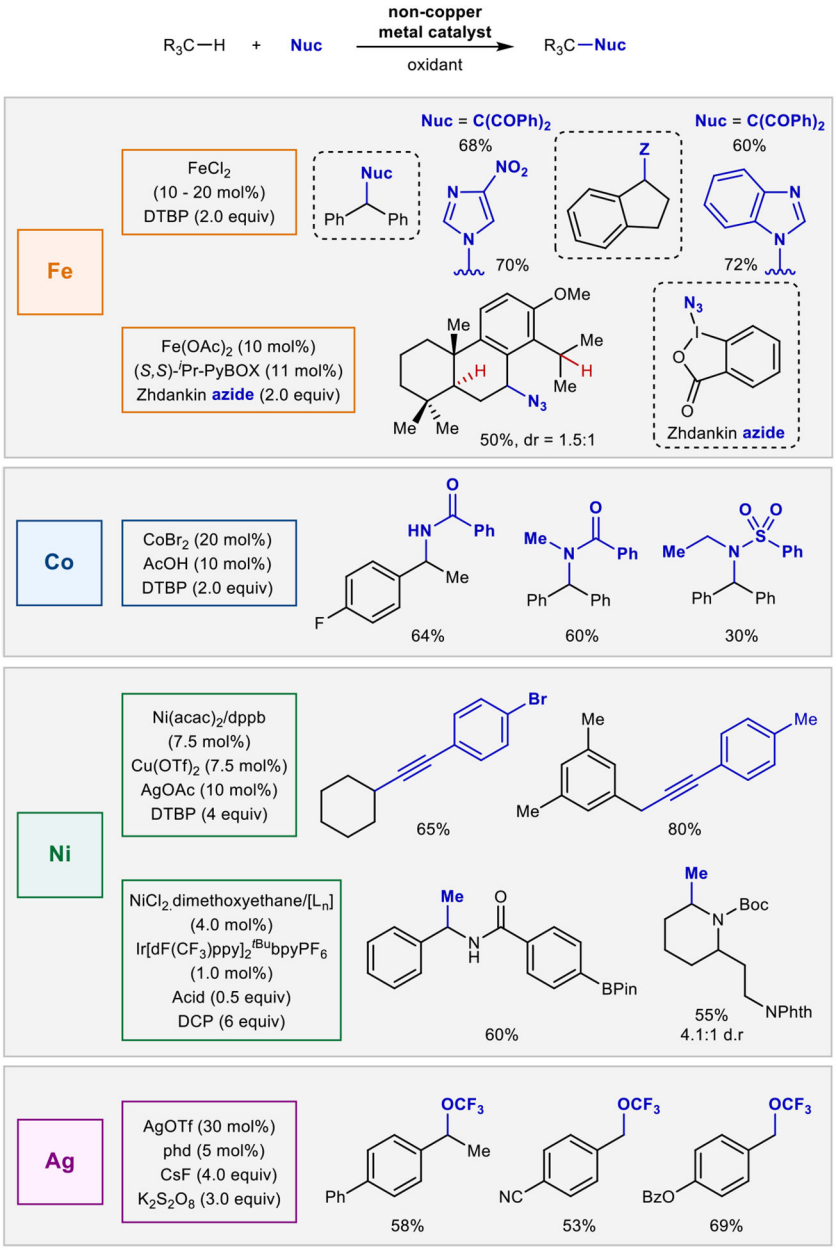

Fig. 7 |. Radical-relay C—H functionalization and cross-coupling reactions with catalysts other than copper.

DTBP, di-*tert*-butyl peroxide; dppb, 1,4-bis(diphenylphosphino)butane; L_n, ligands; DCP, dicumyl peroxide; phd, 1,10-phenanthroline-5,6-dione.

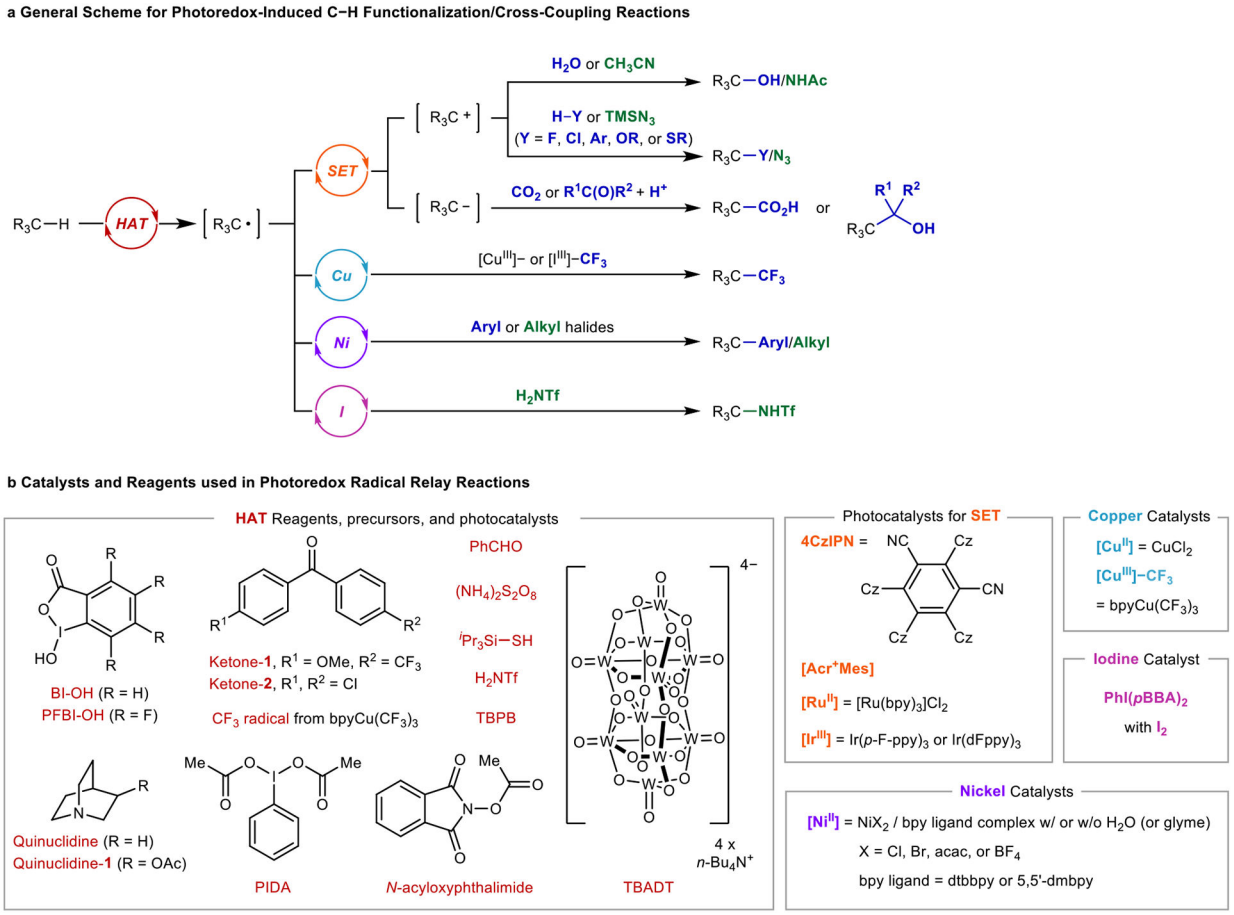

Fig. 8 |. Photoredox C(sp^3)—H functionalization/cross coupling via radical relay.

a | Four pathways for photoredox-promoted C—H functionalization/cross coupling.

b | The photoredox toolbox includes HAT reagents, photocatalysts, and metal-/iodine-based catalysts utilized for representative methodologies. HAT, hydrogen atom transfer; SET, single electron transfer; BI—OH, hydroxyl benziodoxole, PFBI—OH, hydroxyl perfluorobenziodoxole; PIDA, phenyliodonium diacetate; TBADT, tetra-*n*-butylammonium decatungstate; TBPB, *tert*-butyl peroxybenzoate; 4CzIPN, 2,4,5,6-tetra(carbazole-9-yl)isophthalonitrile; [Acr^+Mes], 9-mesityl-1,3,6,8-tetramethoxy-10-phenylacridin-10-ium tetrafluoroborate; bpy, 2,2'-bipyridine; PhI(*p*BBA)$_2$, bis(4-bromobenzoyloxy)iodobenzene; *p*-F-ppy, 5-fluoro-2-(2-pyridinyl-κN)phenyl-κC; dFppy, 2-(2,4-difluorophenyl)pyridine; dtbbpy, 4,4'-di-*tert*-butyl-2,2'-bipyridyl; 5,5'-dmbpy, 5,5'-dimethyl-2,2'-bipyridyl.

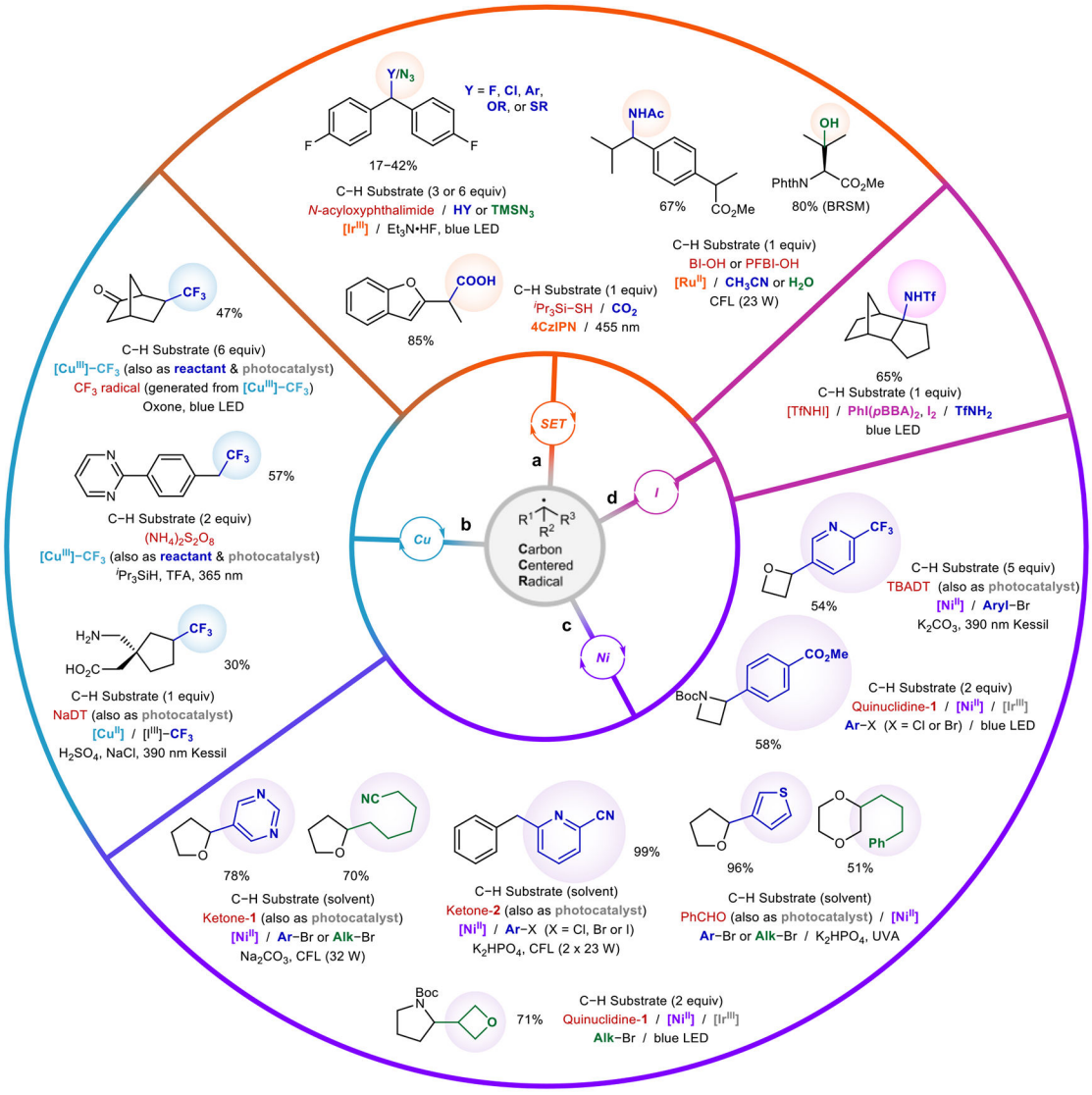

Fig. 9 | Different methods for radical-relay C(sp^3)—H functionalization and cross coupling using carbon-centered radicals access via photoredox methods.

a | Photoredox-promoted C—H functionalization/cross-coupling reactions involving single electron transfer. **b** | Photoredox-promoted C—H functionalization/cross-coupling reactions involving copper catalysts. **c** | Photoredox-promoted C—H functionalization/cross-coupling reactions involving nickel catalysts. **d** | Photoredox-promoted C—H functionalization/cross-coupling reactions involving iodine-based catalysts . SET, single electron transfer; PhI(pBBA)$_2$, bis(4-bromobenzoyloxy)iodobenzene; BI–OH, hydroxyl benziodoxole, PFBI–OH, hydroxyl perfluorobenziodoxole; TFA, trifluoroacetic acid, TBADT, tetra-*n*-butylammonium decatungstate; NaDT, sodium decatungstate; Ketone-1, 4-methoxy-4'-trifluoromethylbenzophenone; Ketone-2, 4,4'-dichlorobenzophenone, BRSM, based on recovered starting material.

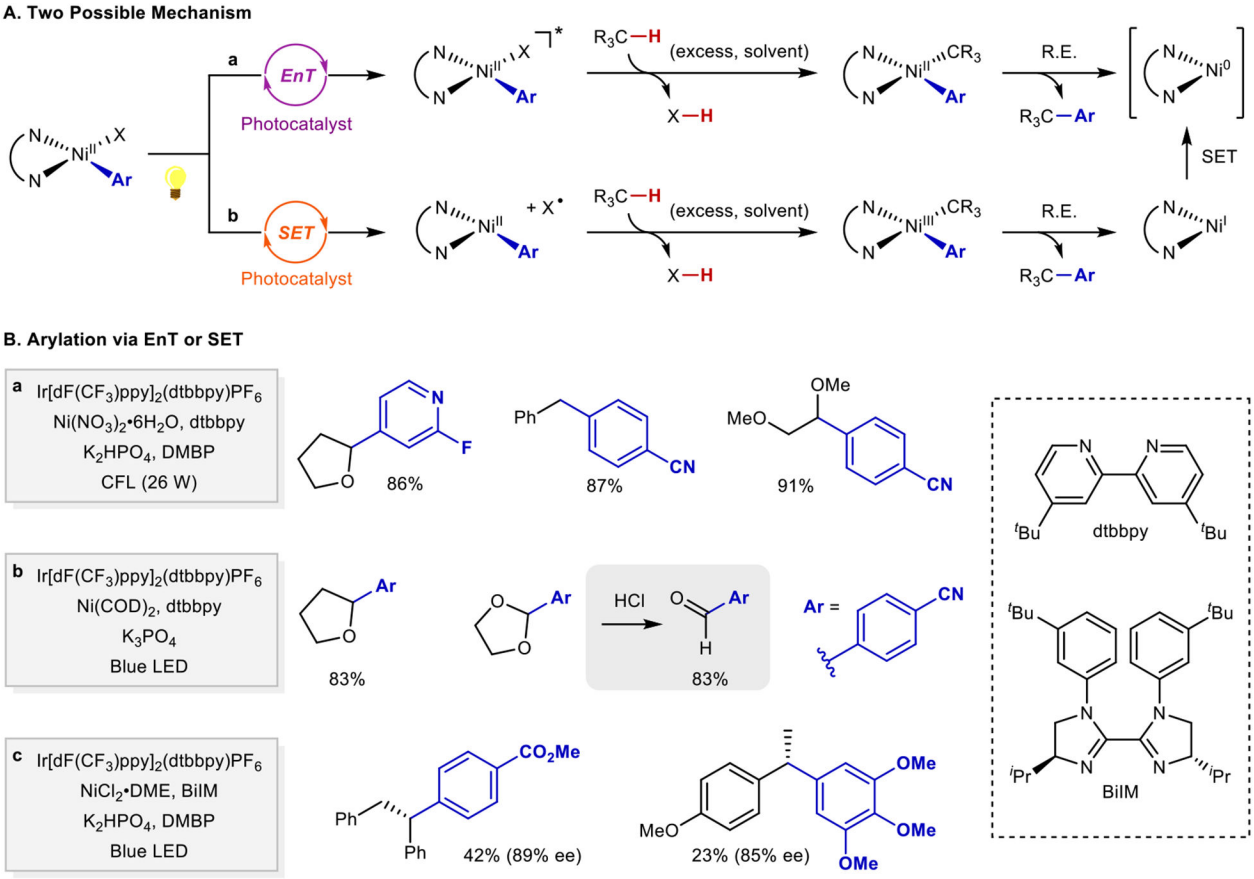

Fig. 10 | Nickel-catalyzed arylation of C(sp^3)—H bonds of inexpensive (co)solvents enabled by *in situ* generation of HAT reagents.

Aa | Energy transfer pathway for arylation of C(sp^3)—H bonds. **Ab** | Single electron transfer pathway for arylation of C(sp^3)—H bonds. **Ba** | Examples of arylated products involving energy transfer. **Bb** | Examples of arylated product involving single electron transfer. **Bc** | Enantioselective arylation of benzylic C(sp^3)—H bonds with a chiral bis-imidazoline ligand. EnT, energy transfer; SET, single electron transfer; R.E., reductive elimination; dF(CF_3)ppy, 3,5-difluoro-2-[5-(trifluoromethyl)-2-pyridinyl]phenyl; dtbbpy, 4,4'-di-*tert*-butyl-2,2'-dipyridyl; BiIM, biimidazoline; DMBP, 4,4'-dimethoxybenzophenone.

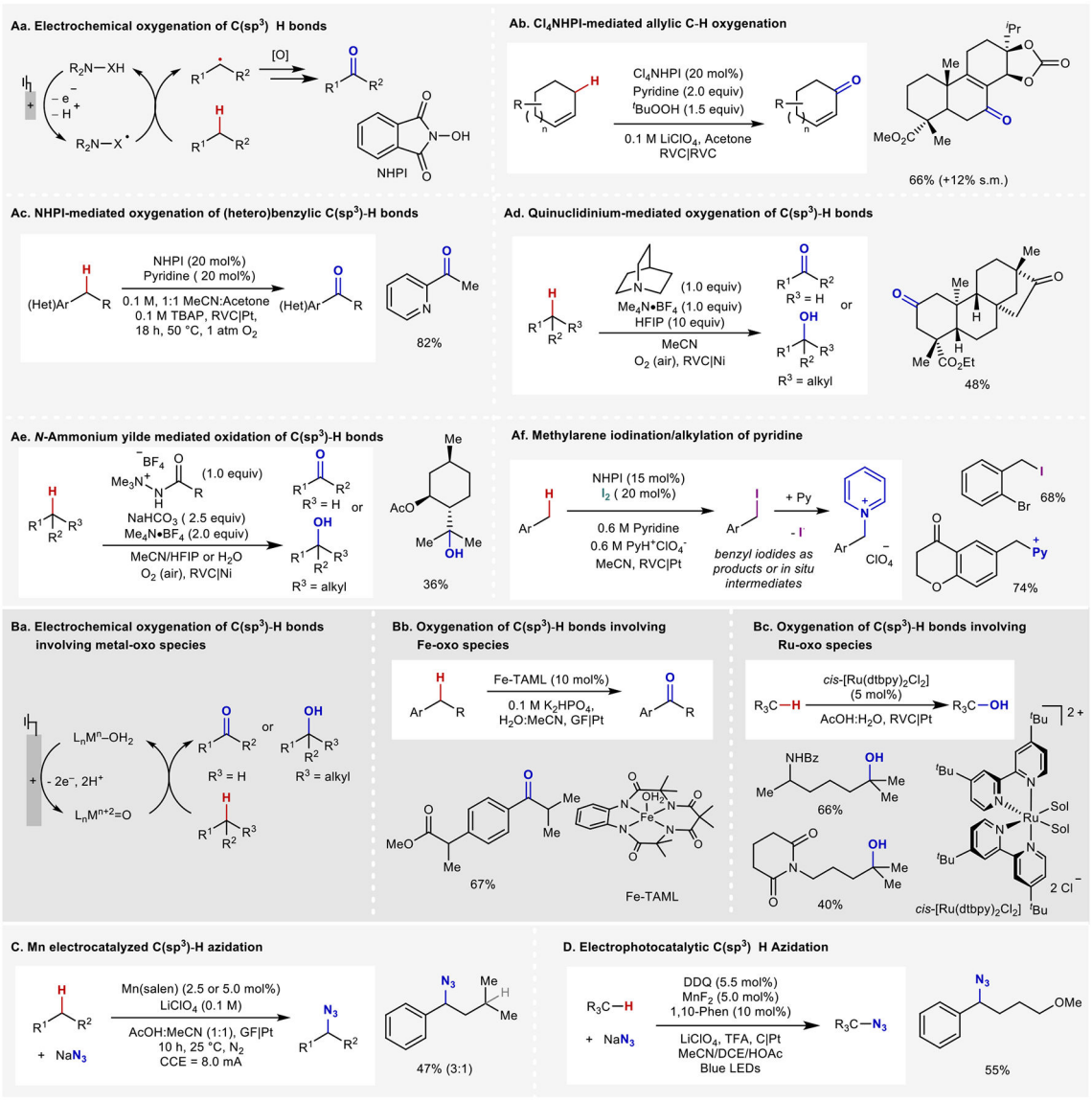

Fig. 11 | . Radical-relay reactions involving electrochemistry.

Aa | General mechanism for NHPI-mediated electrochemical oxygenation reaction of C(sp^3)—H bonds. **Ab** | Oxygenation of allylic C—H bonds. **Ac** | Oxygenation of heterobenzylic C(sp^3)—H bonds. **Ad** | Quinuclidine-mediated oxygenation of C(sp^3)—H bonds. **Ae** | *N*-alkyl ammonium ylides as a new class of HAT-mediators. **Af** | NHPI-mediated iodination followed by pyridination of alkylarenes. **Ba** | Oxygenation reactions involving metal-oxo complexes. **Bb** | Oxygenation of secondary benzylic C(sp^3)—H bonds using Fe-TAML complex. **Bc** | Hydroxylation of C(sp^3)—H bonds in amine derivatives using a ruthenium-based catalyst. **C** | Azidation of C(sp^3)—H bonds using Mn^{III} catalyst. **D** | Photoelectrochemical azidation reaction of C(sp^3)—H bonds. NHPI, *N*-hydroxyphthalimide; Cl_4NHPI, tetrachloro-*N*-hydroxyphthalimide; RVC, reticulated vitreous carbon; TBAP, tetrabutylammonium perchlorate; TAML, tetraamido macrocylic ligand; dtbpy, 4,4'-di-

tert-butyl-2,2'-dipyridyl; DDQ, 2,3-dichloro-5,6-dicyano-p-benzoquinone; 1,10-Phen, 1,10-phenanthroline; TFA, trifluoroacetic acid.